Inherited Depositional Topography Control on Shelf-Margin Oversteepening, Readjustment, and Coarse-Grained Sediment Delivery to Deep Water, Magallanes Basin, Chile

Dustin B. Bauer[1,2], Stephen M. Hubbard[1]*, Jacob A. Covault[3] and Brian W. Romans[4]

[1] Department of Geoscience, University of Calgary, Calgary, AB, Canada, [2] Chevron Canada Limited, Calgary, AB, Canada, [3] Bureau of Economic Geology, Jackson School of Geosciences, The University of Texas at Austin, Austin, TX, United States, [4] Department of Geosciences, Virginia Tech, Blacksburg, VA, United States

A shelf-margin depositional system is the stratigraphic product of terrigenous sediment delivery to the ocean, comprising a flat to low-gradient shelf, or topset, which transitions to a steeper deep-water slope, and, ultimately, a relatively flat basin floor, or bottomset. Erosional and depositional processes across these physiographic domains approximate a clinoform in the stratigraphic record. The shelf margin is a critical environment for terrigenous sediment dispersal because it is a process-regime boundary that links the shelf to deep water and is a marker of basin evolution through time. Additionally, the coarse-grained deposits of strata associated with the shelf-margin zone are important subsurface reservoirs or aquifers. Here, we characterize the shelf-margin and upper slope stratigraphy of the outcropping Upper Cretaceous Tres Pasos and Dorotea formations, Magallanes Basin, southern Chile. The Late Cretaceous Magallanes retroarc foreland basin was an elongate trough oriented parallel to the southern Andean arc and fold-and-thrust belt. The Tres Pasos and Dorotea formations record southward (basin axial) progradation of a high-relief shelf and slope system (>1000 m paleo-water depth) represented by a stratigraphic succession up to 3 km thick that is exposed for tens of kilometers along depositional dip. The character and distribution of deposits that define shelf margins contain evidence for a variety of processes related to deposition, erosion, sediment bypass, and mass wasting. The overall architecture of the Magallanes Basin strata is indicative of a graded shelf-margin system interrupted by periods of slope oversteepening and development of out-of-grade conditions. These punctuated periods are recognized by sedimentological evidence for enhanced bypass of coarse-grained sediment across the upper slope, and thick submarine fan successions in more distal segments. Development of oversteepened depositional topography is particularly significant as it instigated the only two major periods of coarse-grained sediment delivery to deep water over ~8 Myr during the Campanian. The controls on sediment dispersal beyond the shelf margin are commonly discussed in terms of allogenic forcings, such as tectonics, climate, eustasy, and receiving-basin geometry, as well as autogenic behavior,

such as delta-lobe switching. However, inherited depositional topography does not clearly fit within an allogenic/autogenic dichotomy. Depositional topography inherited from shelf-margin evolution influences the position of subsequent shelf margins, which can promote coarse-grained sediment delivery to deep water.

Keywords: stratigraphy, clinoform, basin evolution, clastic sedimentology, Magallanes Basin

INTRODUCTION

A shelf-margin is characterized in depositional-dip profile from shallow-dipping topset, across steeper foreset (clinoform), to shallow-dipping bottomset (**Figure 1**). Shelf-margin profiles that approximate clinoforms are generally considered to represent progradation of graded slopes (Hedberg, 1970; Ross et al., 1994; Steel and Olsen, 2002; Johannessen and Steel, 2005; Patruno et al., 2015; Hodgson et al., 2018). Graded margins are defined as margins where erosional and depositional processes are in equilibrium, resulting in topographically smooth slope profiles that prograde basinward (Hedberg, 1970; Ross et al., 1994). Conversely, Hedberg (1970) described out-of-grade slopes, wherein the shelf margin and upper slope are zones of net erosion, sediment bypass, and mass wasting, whereas the lower slope and basin are associated with substantial deposition. The shelf margin is a gateway for the transport of coarse-grained sediment into deep water, and it is commonly attributed to either external forcings (i.e., allogenic controls) promoting sediment supply (Carvajal and Steel, 2009; Kertznus and Kneller, 2009) or internal dynamics of the system (i.e., autogenic controls), such as compensational stacking as a result of delta-lobe switching (Olariu and Bhattacharya, 2006; Muto et al., 2007; Straub et al., 2009; Hajek and Straub, 2017). Ross et al. (1994) noted that inherited depositional topography can control the evolution of later shelf margins, potentially fostering development of oversteepened upper slopes and promoting mass wasting and/or coarse-grained sediment delivery to deep water (**Figure 1**). Inherited depositional topography does not clearly fit into the either/or, allogenic/autogenic dichotomy of controls on shelf-margin depositional evolution because underlying deposits might have been the product of a wholly distinct set of conditions.

Studies of shelf-margin depositional systems have commonly focused on the prediction of down-slope deep-water fans through stratigraphic analysis (Plink-Björklund et al., 2001; Prather et al., 2017), analysis of external controls (Carvajal and Steel, 2009), or investigation of shelf-edge deposits (i.e., wave-, tide-, or river-dominated process regime) (e.g., Dixon et al., 2012b; Cosgrove et al., 2018). The controls on transitions between slopes with a graded profile and out-of-grade configurations that promote coarse-grained sediment transfer to deep water have remained understudied (Gomis-Cartesio et al., 2018). Slope readjustment comprises the processes of erosion, sediment bypass, and marine onlap of submarine-fan deposits in response to changing basin physiography (Ross et al., 1994). However, the detailed sedimentology and stratigraphy of major shelf-margin readjustments, like those described by Ross et al. (1994) across a large-scale shelf-margin transect, have not been well documented. Furthermore, comparably little work has been focused on the
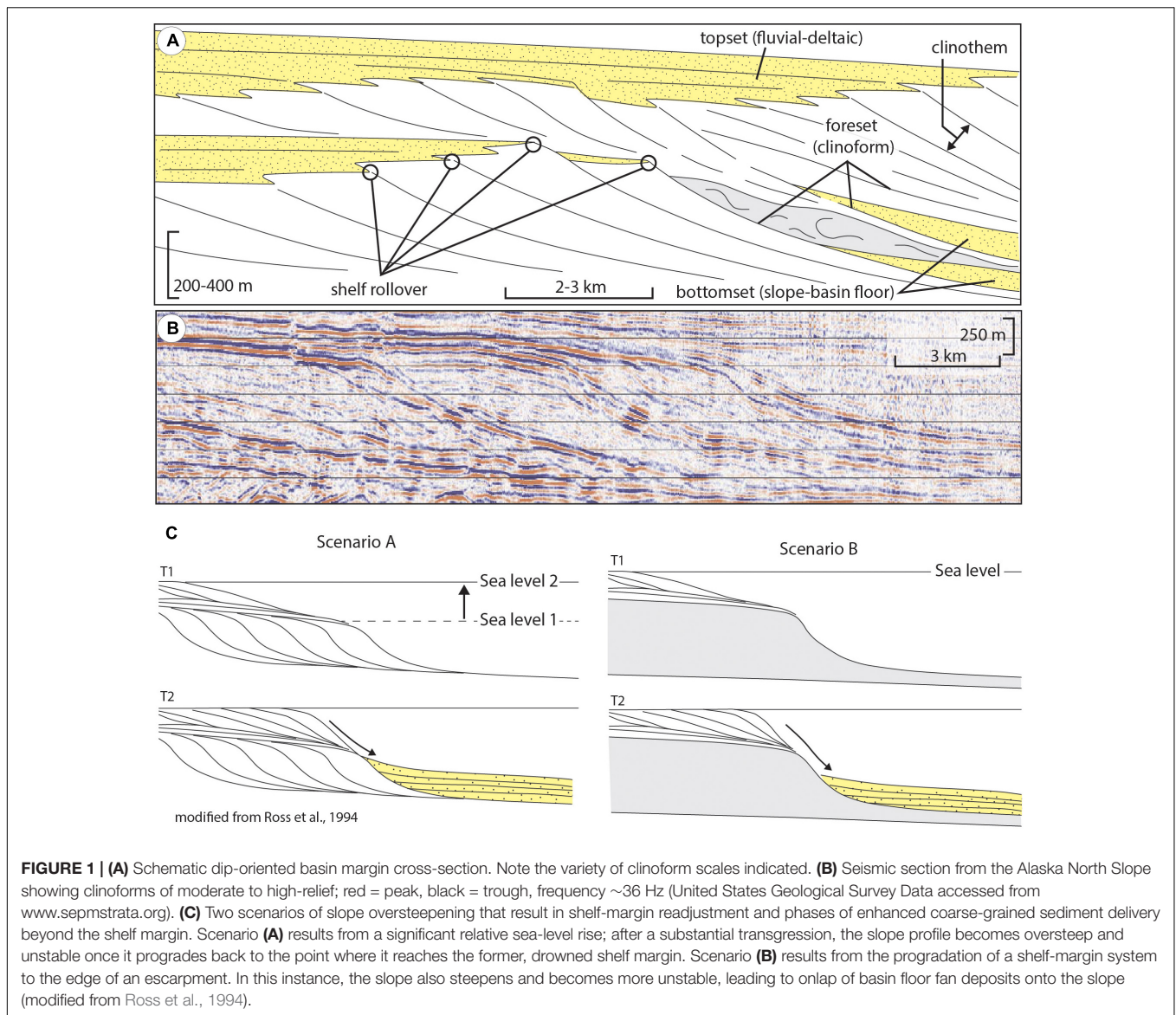
sedimentologic record along the entirety of the transition from shallow-marine to deep-water depocenters along basin margins of high relief (>500 m) (Dixon et al., 2012a; Poyatos-Moré et al., 2019). Deciphering the details of siliciclastic basin margins is challenging as a result of their large scale (several hundreds of meters to kilometers of relief; McMillen, 1991; Helland-Hansen, 1992; Hubbard et al., 2010; Patruno et al., 2015). These high-relief shelf-margin systems are most commonly observed in seismic-reflection data, characterized by >10 m of vertical resolution (e.g., Pinous et al., 2001; Houseknecht et al., 2009), with important insight drawn from stratigraphic modeling (e.g., Uličný et al., 2002; Burgess et al., 2008; Gerber et al., 2008).

This study focuses on the characterization of outcropping shelf-margin stratigraphy, with an emphasis on the record of punctuated out-of-grade conditions related to inherited depositional topography in the Upper Cretaceous Tres Pasos and Dorotea formations, southern Chile. The unique outcrop perspective of seismic-scale clinoforms (i.e., >1000 m relief) provides the opportunity to investigate the stratigraphic architecture developed in response to shelf-margin oversteepening. This is augmented with documentation of the down-dip sedimentological variability along out-of-grade surfaces that were associated with significant coarse-grained sediment bypass to the deep basin.

GEOLOGIC SETTING

In this study, we examine deposits of the Upper Cretaceous Dorotea and Tres Pasos formations that crop out in southern Chile (**Figure 2**; Hubbard et al., 2010; Daniels et al., 2018). The units were deposited in the Cenomanian–Maastrichtian Magallanes retroarc foreland basin, located at the southern end of the 7000 km-long Andean Cordillera along the southwestern margin of the South American plate (**Figure 2A**; Dalziel, 1981; Wilson, 1991; Fildani and Hessler, 2005; Daniels et al., 2019).

The Magallanes Basin contains 3–5 km of Upper Cretaceous deep-water strata, deposited during a prolonged period of elevated subsidence (Romans et al., 2011; Bernhardt et al., 2012). The foreland basin is underlain by thinned continental crust, attributed to a precursor extensional back-arc basin (Rocas Verdes Basin; Romans et al., 2010; Fosdick et al., 2011). This attenuated continental crust promoted high subsidence during thrust loading and led to long-lived deep-water conditions in the retroarc setting (Natland et al., 1974; Hubbard et al., 2010; Fosdick et al., 2014). Deposition of unconfined turbidites of the Cenomanian-Turonian Punta Barrosa Formation marks the onset of deep-water sedimentation (Fildani et al., 2003; Malkowski et al., 2017), followed by the Coniacian-early

FIGURE 1 | (A) Schematic dip-oriented basin margin cross-section. Note the variety of clinoform scales indicated. **(B)** Seismic section from the Alaska North Slope showing clinoforms of moderate to high-relief; red = peak, black = trough, frequency ~36 Hz (United States Geological Survey Data accessed from www.sepmstrata.org). **(C)** Two scenarios of slope oversteepening that result in shelf-margin readjustment and phases of enhanced coarse-grained sediment delivery beyond the shelf margin. Scenario **(A)** results from a significant relative sea-level rise; after a substantial transgression, the slope profile becomes oversteep and unstable once it progrades back to the point where it reaches the former, drowned shelf margin. Scenario **(B)** results from the progradation of a shelf-margin system to the edge of an escarpment. In this instance, the slope also steepens and becomes more unstable, leading to onlap of basin floor fan deposits onto the slope (modified from Ross et al., 1994).

Campanian Cerro Toro Formation, a mudstone-dominated succession with a conglomeratic channel system situated along the length of the foredeep axis (**Figure 2D**; Crane and Lowe, 2008; Hubbard et al., 2008; Jobe et al., 2010). The subsidence rate waned and the basin underwent a ~2 Myr long period during which mass-failure processes dominated, presumably due to a change in hinterland dynamics and/or basin uplift (Daniels et al., 2018, 2019). Subsequently, the basin filled with the Campanian-Maastrichtian Tres Pasos and Dorotea formations, characterized by shelf-margin clinoforms that prograded along the basin axis, from north to south (Romans et al., 2009; Hubbard et al., 2010; Schwartz and Graham, 2015). The Tres Pasos Formation is a mudstone-dominated slope succession with intercalated sandy turbidite systems and mass-transport deposits (Smith, 1977; Shultz et al., 2005; Armitage et al., 2009; Auchter et al., 2016); these strata are overlain by genetically linked deltaic deposits of the Dorotea Formation (Arbe and Hechem, 1984;

Macellari et al., 1989; Covault et al., 2009; Hubbard et al., 2010; Leppe et al., 2012; Schwartz and Graham, 2015; Schwartz et al., 2017; Manriquez et al., 2019). The deep-water basin (>1000 m relief) and basin axially oriented depositional systems (>40 km long slopes) promoted the development of shelf-margin clinoforms similar in scale to those of continental margins (**Figures 2E,F**; Carvajal and Steel, 2009; Hubbard et al., 2010; Romans et al., 2011).

METHODOLOGY

The study area is located at approximately 51° 00′ S and 72° 30′ W, adjacent to the Chile-Argentina border (**Figure 2**). We focus on a 15 km-long exposure of a high-relief shelf-margin depositional system at Cerro Cazador (**Figure 2C**). At this location, we record south-southeast paleoflow, which is
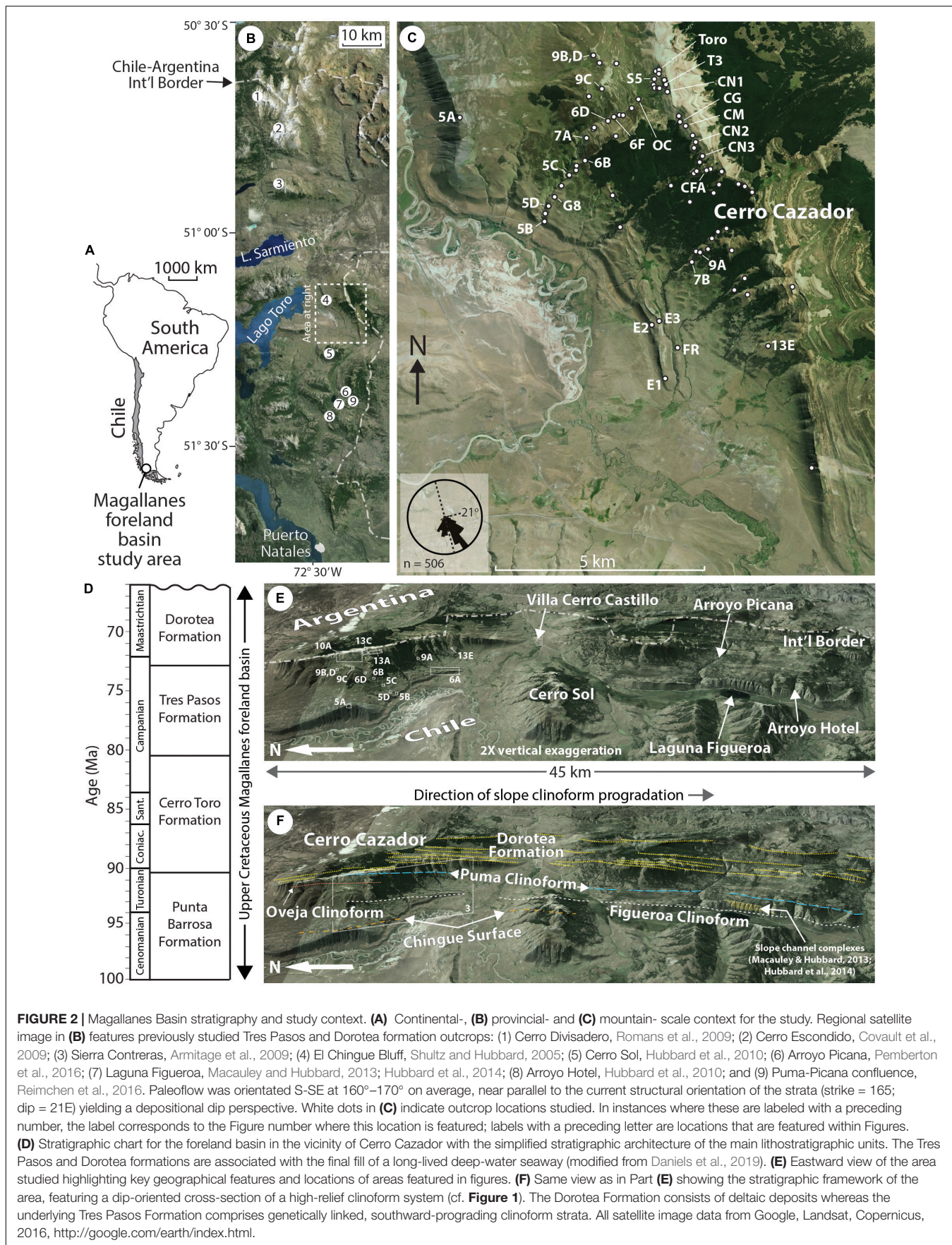
FIGURE 2 | Magallanes Basin stratigraphy and study context. **(A)** Continental-, **(B)** provincial- and **(C)** mountain- scale context for the study. Regional satellite image in **(B)** features previously studied Tres Pasos and Dorotea formation outcrops: (1) Cerro Divisadero, Romans et al., 2009; (2) Cerro Escondido, Covault et al., 2009; (3) Sierra Contreras, Armitage et al., 2009; (4) El Chingue Bluff, Shultz and Hubbard, 2005; (5) Cerro Sol, Hubbard et al., 2010; (6) Arroyo Picana, Pemberton et al., 2016; (7) Laguna Figueroa, Macauley and Hubbard, 2013; Hubbard et al., 2014; (8) Arroyo Hotel, Hubbard et al., 2010; and (9) Puma-Picana confluence, Reimchen et al., 2016. Paleoflow was orientated S-SE at 160°–170° on average, near parallel to the current structural orientation of the strata (strike = 165; dip = 21E) yielding a depositional dip perspective. White dots in **(C)** indicate outcrop locations studied. In instances where these are labeled with a preceding number, the label corresponds to the Figure number where this location is featured; labels with a preceding letter are locations that are featured within Figures. **(D)** Stratigraphic chart for the foreland basin in the vicinity of Cerro Cazador with the simplified stratigraphic architecture of the main lithostratigraphic units. The Tres Pasos and Dorotea formations are associated with the final fill of a long-lived deep-water seaway (modified from Daniels et al., 2019). **(E)** Eastward view of the area studied highlighting key geographical features and locations of areas featured in figures. **(F)** Same view as in Part **(E)** showing the stratigraphic framework of the area, featuring a dip-oriented cross-section of a high-relief clinoform system (cf. **Figure 1**). The Dorotea Formation consists of deltaic deposits whereas the underlying Tres Pasos Formation comprises genetically linked, southward-prograding clinoform strata. All satellite image data from Google, Landsat, Copernicus, 2016, http://google.com/earth/index.html.
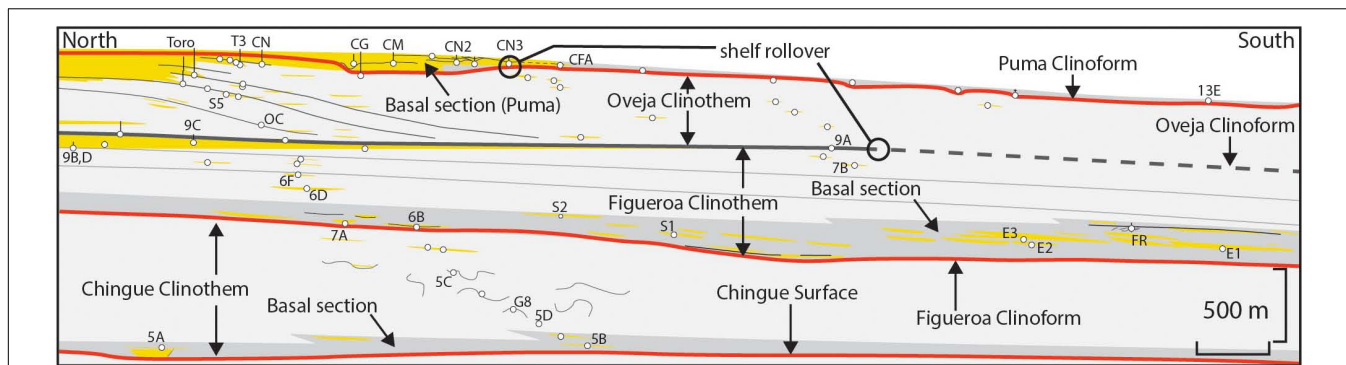
FIGURE 3 | Simplified depositional dip-oriented stratigraphic cross-section constructed from outcrop observations at Cerro Cazador (see **Figures 2E, 4** for transect location). The main stratigraphic components and outcrop locations provide context for outcrop descriptions and interpretations. Note that thin vertical lines indicate locations of particularly long (>25 m) detailed measured sections. In general, sandstone-dominated strata are yellow and siltstone-dominated clinothem packages are gray; basal clinothem packages emphasized with a darker shade of gray. Thick, bold lines (red and dark gray) are interpreted clinoforms.
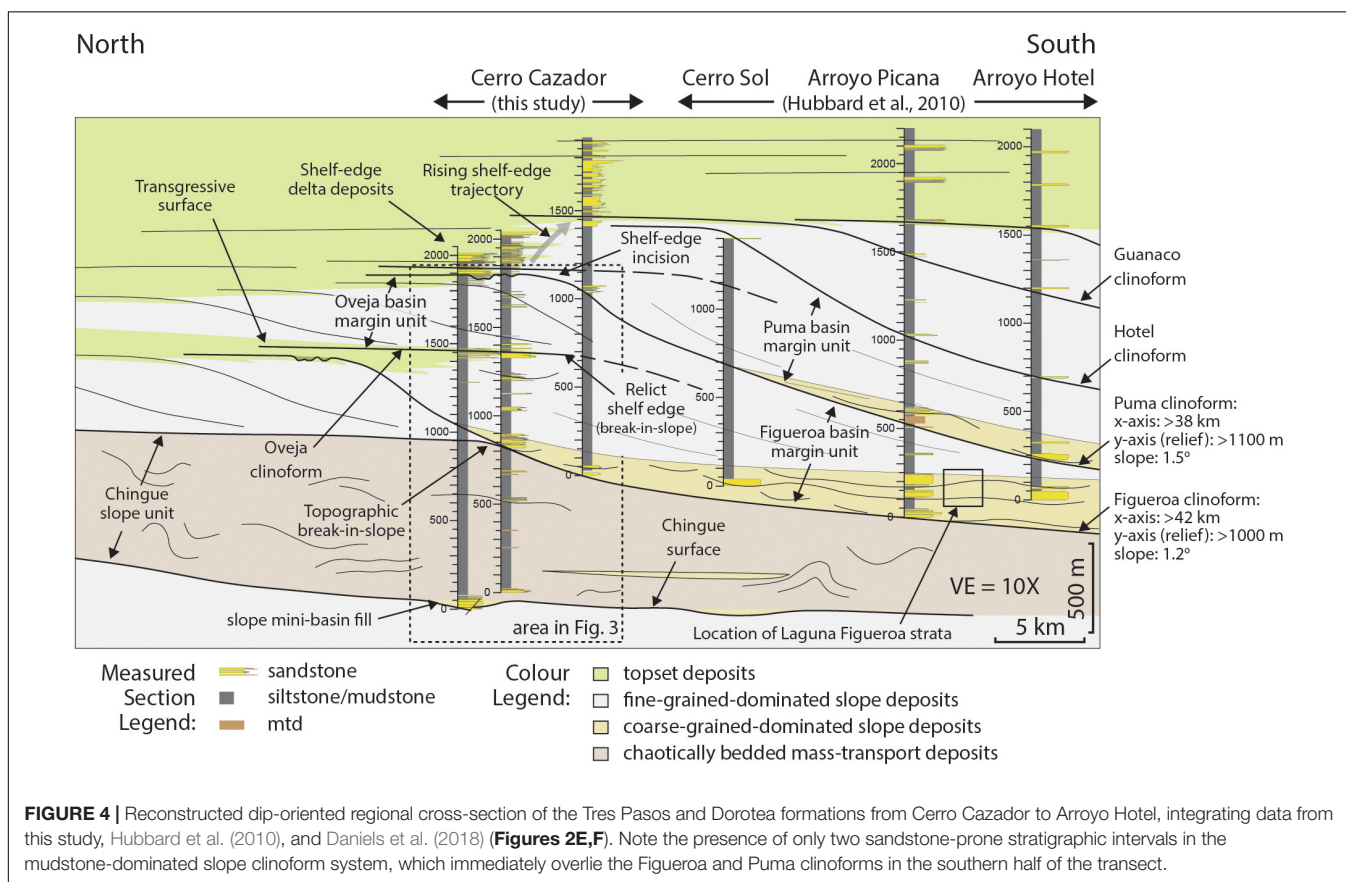
FIGURE 4 | Reconstructed dip-oriented regional cross-section of the Tres Pasos and Dorotea formations from Cerro Cazador to Arroyo Hotel, integrating data from this study, Hubbard et al. (2010), and Daniels et al. (2018) (**Figures 2E,F**). Note the presence of only two sandstone-prone stratigraphic intervals in the mudstone-dominated slope clinoform system, which immediately overlie the Figueroa and Puma clinoforms in the southern half of the transect.

approximately parallel to the N/NW-S/SE south trend of the outcrop (**Figure 2C**; Smith, 1977; Shultz and Hubbard, 2005; Bauer, 2012; Daniels et al., 2018). The correlation between deltaic and slope strata can be physically traced in the outcrop belt over several kilometers in many cases (**Figures 2F, 3, 4**). Relatively flat strata of the upper part of the Dorotea Formation at the top of the succession are preserved across the entire study area and are used as a datum, providing the basis for estimations of shelf-margin relief.

High-resolution satellite imagery draped on a digital elevation model was used to correlate the outcrop to the regional stratigraphic framework of Hubbard et al. (2010) to the south, which comprises a series of southward-prograding clinoforms and clinothems >35 km long and 900–1000 m thick (**Figures 2E,F**). Hubbard et al. (2010) were the first to interpret these clinoforms by tracing the base of thick (40–100 m), sandstone-rich packages exposed as prominent ridges 10–35 km long in the outcrop belt. These composite

sandy units are described as "basal clinothem packages" in this study, which directly overlie erosional surfaces that share characteristics of sequence boundaries (Mitchum et al., 1977; Houseknecht et al., 2009). Although clinoforms can be defined by relatively continuous shelf-margin mudstone-prone strata that potentially represent zones of maximum flooding (Galloway, 1989; Steel et al., 2008; Houseknecht et al., 2009), the large scale of the Tres Pasos-Dorotea clinoforms in the Magallanes Basin and sparse exposure of vegetated mudstone-prone strata make delineation of flooding surfaces unreliable over long distances. As such, it is likely that many more clinoforms are present in the outcrop belt than are detected and reported here; the identified clinoforms likely bound multiple clinothems (e.g., Patruno et al., 2015). Thus, these strata could be considered as clinothem sets or compound clinothems, but for simplicity we refer to them as clinothems throughout.

The dataset collected for this study includes 2980 m of measured stratigraphic section, which represents the foundation for facies analysis. Facies variations along individual clinoforms are documented from measurements of grain size, sedimentary structures, bed contacts, and trace fossils (summarized in **Table 1**). Detailed stratigraphic correlations are made by physically tracing surfaces as well as beds, and confirmed through the use of ground-based and aerial photo mosaics. Where tracing surfaces is not possible due to inaccessible topography, regional correlations (5–40 km) are made with high-resolution satellite data (<1 m resolution).

TRES PASOS AND DOROTEA STRATIGRAPHY AND SEDIMENTOLOGY

Regionally, the fill of the Magallanes Basin is characterized by southward prograding shelf-margin strata exposed for >100 km north-south distance (Romans et al., 2010; Daniels et al., 2018). We consider the clinoforms to be high relief, based on comparison to the compilation of Carvajal et al. (2009). In this section, we describe and interpret key characteristics of the Tres Pasos-Dorotea shelf-margin system, aspects of which were first broadly presented by Hubbard et al. (2010). Key components are the 40–100 m-thick basal clinothem packages (**Figure 3**), which variably extend at least tens of kilometers from Cerro Cazador (north) to Arroyo Hotel (south) (**Figure 4**). These sandstone-rich basal packages are overlain by fine-grained successions hundreds of meters thick, which compose the bulk of clinothem strata. Toward the north, clinothems are capped by resistant sandstone-rich (topset) deposits; these deposits generally pinch out southward (basinward).

The strata include a section of thick, mass-transport-deposit (MTD)-dominated strata (Chingue unit), and three shelf-margin units (i.e., Figueroa, Oveja, and Puma; **Figure 3**). The MTD-dominated Chingue unit and the progressively younger shelf-margin units (Figueroa through Puma) correspond to the four stages of basin evolution described by Daniels et al. (2018). Although the shelf-margin strata correlates farther to the south, our emphasis on clinothems associated with abundant slope

sandstone focused our analysis on the Figueroa and Puma shelf-margin units (**Figure 4**). Due to the large scale of the shelf-margin strata and limited outcrop extent, only the youngest shelf-margin units (upper Figueroa, Oveja, and Puma) are exposed from topset through distal slope; the bases of the Figueroa and Chingue units are characterized exclusively by slope strata in the portion of the outcrop belt studied. There is a lack of evidence for unconfined submarine fan deposits at the distal end of the outcrop belt. It is plausible that unconfined deposits have not been encountered because a significant toe-of-slope break at the transition to the basin floor did not exist in the basin; both non- and deep-marine foreland basins commonly promote formation of long channel systems due to a preferred tectonic slope along their axes, as well as lateral confinement (e.g., Graham et al., 1975; Burbank, 1992; Malkowski et al., 2017; Sharman et al., 2018).

Like other outcrops of large-scale shelf-margin systems, the Tres Pasos-Dorotea deposits at Cerro Cazador provide primarily a two-dimensional (2-D) perspective of the ancient basin margin, limiting interpretations of stratigraphic evolution in 3-D. Considerable along-strike variability of continental margins on the modern seafloor (e.g., Olariu and Steel, 2009; Ryan W. B. et al., 2009) suggests that the same variation ought to be expected in the stratigraphic record of the Magallanes foreland basin margin (e.g., Martinsen and Helland-Hansen, 1995; Driscoll and Karner, 1999; Jones et al., 2015; Madof et al., 2016; Paumard et al., 2018; Poyatos-Moré et al., 2019).

The Chingue Unit

The Chingue deep-water unit is up to 900 m thick and exposed for 5 km along depositional dip (**Figure 4**). Due to the large thickness and areal extent of the stratigraphic unit, deposits of only a relatively short segment of the entire paleo-slope crop out at Cerro Cazador. A basal sandstone-rich Chingue stratigraphic package is 50–75 m thick (**Figure 3**) and consists of an upward coarsening and bed thickening succession (Facies F1, F3–5; **Figures 5A,B**) capped by a chaotically bedded deposit (Facies F2) and a sandstone-filled channel form (Facies F3; **Table 1**). The basal sandstone-rich Chingue stratigraphic package is lenticular in a depositional-dip perspective, and overlies a zone of growth faulting and abundant sandstone intrusions (**Figure 5A**). Overlying this basal package is ∼800 m of chaotically bedded strata (**Figure 4**).

Shultz and Hubbard (2005) attribute the basal sandstone-rich package of the Chingue deep-water unit to ponding in localized accommodation created by growth faulting on an unstable slope. The capping MTD and channel fill are interpreted to record healing of the accommodation and basinward stepping of a channel system down slope (cf. transient fan of Adeogba et al., 2005). Overlying this basal sandstone-rich section, the hundreds of meters of chaotically bedded deposits are attributed to long-lived mass wasting (Facies F2; **Figures 5C,D**; **Table 1**; Daniels et al., 2018). The propensity of MTDs is interpreted to record an extended period of out-of-grade slope processes, during which the upper slope was oversteepened and prone to regular failure (**Figure 4**; Ross et al., 1994; Prather et al., 2017). These MTD-dominated strata reach their maximum thickness at Cerro Cazador and thin southward (**Figure 4**).

TABLE 1 | Facies of the Tres Pasos and Dorotea formations at Cerro Cazador.

	Facies	Texture	Thickness	Physical structures	Grading	Sorting	Basal contact	Bed geometry	Lithological accessories	Trace fossils	BI	Trace fossil size and abundance	Interpretation
F1	Carbonaceous mudstone	siltstone and clay	3-400 cm	Planar laminae	None	Moderate-well	Gradational	Extensive 100's of meters	Organic detritus	*Th, Pl, Sk*	0–3	Small, rare	Low density gravity flow and suspension deposits
F2	Chaotically bedded sandstone and mudstone	fg ss, siltstone and clay	<10 m	Overturned and contorted beds, rare planar laminae	None	Poor-moderate	Discordant	Rafted siltstone blocks, lenticular sandstone beds, laterally extensive to locally contorted units	Organic detritus	np	0	np	Mass transport, including cohesive debris flow deposits
F3	Amalgamated sandstone	cg to mg ss with granules and pebbles	5–130 cm	Massive, planar laminae, asymmetrical ripple cross-stratification	Normal	Poor-moderate	Erosive 3–50 cm relief	Channelized 5–50 m	Mudstone intraclasts, rare shell molds	np	0	np	Traction deposits; high density turbulent flows
F4	Tabular non-amalgamated sandstone	cg to vfg ss with rare granules	1–105 cm	Planar stratification, asymmetrical ripple cross-stratification	Normal	moderate	Flat/sharp	Laterally extensive (up to 75 m) some beds thin laterally over 10–25 m	Rare mudstone intraclasts, organic detritus	*Sk, Th, Pl, Op*	0–2	Small to moderate, rare	Laterally extensive high to low density turbidites
F5	Lenticular non-amalgamated sandstone	cg to vfg ss with rare granules	1–150 cm	Planar stratification, asymmetrical ripple cross-stratification	Normal	moderate	Flat to erosive <5 cm relief	Beds thin over 10–75 m	Rare mudstone intraclasts, organic detritus	*Sk, Pl, Gy, Th, Op, He, CH, Ch*	0–2	Small to moderate, rare	Traction deposits; high density turbidites

(Continued)

TABLE 1 | Continued

	Facies	Texture	Thickness	Physical structures	Grading	Sorting	Basal contact	Bed geometry	Lithological accessories	Trace fossils	BI	Trace fossil size and abundance	Interpretation
F6	TCS lenticular sandstone	mg to fg	5–100 cm	trough cross-stratification, planar stratification, backset stratification	None to normal at very top	Poor-moderate	flat to erosive <5 cm relief	Lenticular 2–25 m	Rare mudstone intraclasts, organic detritus	*Sk, Pl, Op*	0–1	small, rare	Traction deposits; sustained unidirectional currents
F7	Lenticular sandstone	cg to mg ss with granules and pebbles, rare silt	10–120 cm	Trough cross-stratification, planar stratification, asymmetrical ripple cross-stratification	Normal	Poor-moderate	Erosive 5–100 cm relief	Channelized 10–40 m	Organic detritus, wood and plant debris), mudstone intraclasts	Np	0	np	Traction deposits; unidirectional channel flow
F8	TCS and planar laminated sandstone	cg to fg ss	10-100 cm	Planar stratification, tabular cross-stratification	None to slightly normal	Poor-moderate	Flat/sharp to slightly erosive 0–3 cm relief	Lenticular 10–70 m	Organic detritus, mudstone intraclasts	*Pl, Sk, Op, Gy, Pa, Te, fug*	0–2	Small - robust, rare	Sustained unidirectional flow, dune migration
F9	Hummocky cross-stratified sandstone	mg to fg ss	40–75 cm	Hummocky cross-stratification, symmetrical ripple cross stratification	Normal	Moderate-well	Wavy to flat	Lenticular 10–50 m	Minor organic detritus	np	0	np	Reworking of sediment through oscillatory currents
F10	Deformed sandstone	mg ss to siltstone	2–150 cm	Contorted layers, flames, ball and pillow	None to slightly normal	Moderate	Undulatory and irregular	Lenticular 5–20 m	Organic detritus	np	0	np	Water escape, slumping, loading
F11	Inversely graded sandstone	fg to mg ss	10–20 cm	Flames, ball and pillow	Reverse	Moderate	Flat/sharp	Lenticular 20–50 m	Organic detritus, rare mudstone intraclasts	np	0	np	Waxing gravity flow deposits, loading
F12	Organic rich mudstone and fine-grained sandstone	fg to vfg ss, siltstone and clay	1–100 cm	Planar laminations, asymmetrical ripple cross-stratification	Normal	Moderate	Gradational	Extensive 100's m's	Abundant organic detritus	*Pl, Th, Sk*	0–4	Small, rare to moderate	Low density turbidites and suspension deposits

(Continued)

TABLE 1 | Continued

Facies	Texture	Thickness	Physical structures	Grading	Sorting	Basal contact	Bed geometry	Lithological accessories	Trace fossils	BI	Trace fossil size and abundance	Interpretation
F13 Normally graded sandstone	mg to vfg ss	1–50 cm	Planar stratification, asymmetrical ripple cross-stratification	Normal	Moderate-well	Flat/sharp	lenticular to tabular 10–100 m	Organic detritus	Sk, Pl, Th, Op, Ch	0–3	Small - moderate, rare to moderate	High density gravity flow deposits
F14 Carbonaceous mudstone and mudstone	Carbonaceous siltstone and clay mudstone	1–500 cm	Planar laminae	None	Moderate	Gradational	Extensive 100's m's	Organic detritus	Pl, Th, Sk	0–3	Small, rare to moderate	Low density turbidites and suspension deposits

BI, bioturbation index (cf. MacEachern and Bann, 2008); vfg, very fine-grained; fg, fine-grained; mg, medium-grained; cg, coarse-grained; ss, sandstone; Th, Thalassinoides; Pl, Planolites; Sk, Skolithos; Op, Ophiomorpha; Gy, Gyrolithes; He, Helminthopsis; Pa, Palaeophycus; Te, Teichichnus; Ch, Chondrites; fug, fugichnia; np, not present; TCS, trough cross-stratified.

The Figueroa Shelf-Margin Unit

The Figueroa shelf-margin unit is up to 600–700 m thick and exposed for >40 km along depositional dip (**Figure 4**). The basal Figueroa clinothem package is 75–125 m thick (**Figure 3**), primarily consisting of sandstone-filled channel forms (Facies F3-F4) encased in mudstone (Facies F1) and chaotically bedded deposits (Facies F2) (**Figures 6A–C, 7A**). Channel forms are discontinuously exposed along the dip-oriented outcrop belt (**Figure 6A**). The base of this sandstone-rich succession defines the Figueroa clinoform, which has at least 900–1000 m of relief (**Figures 2F, 4**; Hubbard et al., 2010; Daniels et al., 2018). Although the paleoslope gradient cannot be accurately measured in the uplifted stratigraphic succession, physical correlation in the outcrop belt demonstrates that it is steepest in the most proximal locations preserved (see Cerro Cazador locality in **Figure 4**). The topset deposit is not preserved in the outcrop belt for this clinoform segment.
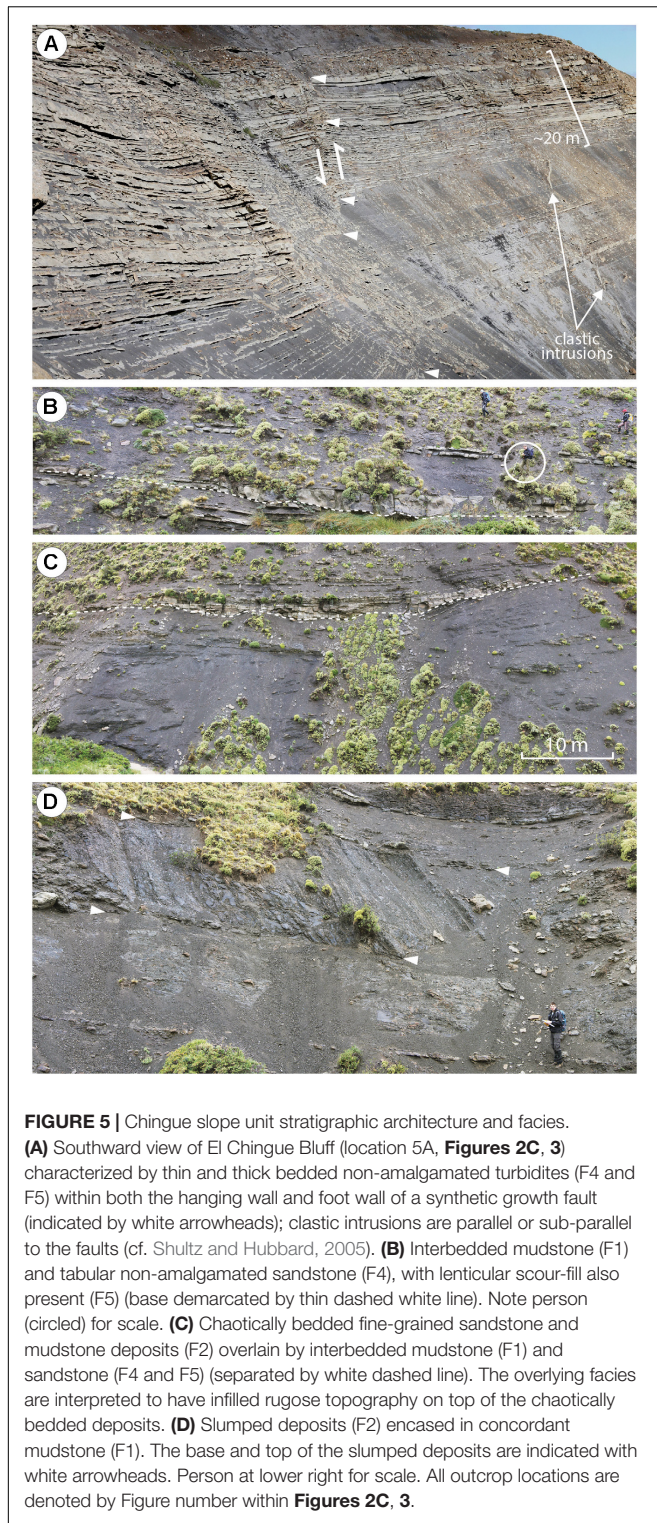
The basal Figueroa clinothem package reflects a transition to increased sand delivery to the slope, supported by the presence of a 300 m-thick section of sandy slope turbidites at Laguna Figueroa (**Figures 4, 8**; Hubbard et al., 2010). We postulate that a southward prograding delta reached the break-in-slope associated with the upper surface of MTD-dominated stratigraphy in the Chingue unit (**Figure 8**). The basin margin was oversteepened, and a prolonged period of coarse-grained sediment transfer off the shelf edge was initiated (cf. Ross et al., 1994; **Figure 1C**). A number of drivers for the sedimentation pattern in the basin could be drawn upon; however, the inherited basin topography evident from the stratigraphic analysis is suggestive that it was a dominant driver of off-shelf delivery of coarse-grained sediment.

The upper part of the Figueroa clinothem, stratigraphically overlying the sandstone-rich basal clinothem package (**Figure 3**), is 300–500 m thick at Cerro Cazador. To the north, it is capped by a series of upward-coarsening packages that are collectively up to 100–150 m thick (Facies F9–10, F12, F14) (**Figure 8** and **Table 1**). These packages pinch-out southward into widespread concordant fine-grained strata with isolated sandstone bodies (Facies F1, F4-F5) (**Figures 6D–F**) and localized MTDs (**Figure 7B**). The coarsening-upward packages are characterized by widespread evidence for shallow-marine conditions, including hummocky cross stratification, symmetrical ripples, abundant wood debris, and a low-diversity trace fossil suite (**Figure 9**; **Table 1**; MacEachern et al., 2005).

Upper Figueroa clinothem stratigraphy is interpreted to record the southward transition of deltaic topset deposits into mudstone-prone prodelta and slope strata (**Figures 3, 4**).

The Oveja Shelf-Margin Unit

The Oveja shelf-margin unit is 300–400 m thick (**Figures 3, 10A–C**), consisting of a 30–50 m thick upper section with 5–20 m thick upward-coarsening and bed-thickening successions with carbonaceous mudstone (F14), lenticular coarse-grained sandstone (F7), medium-grained sandstone (F10, F13), and hummocky cross-stratified sandstone (F9) (**Figures 7C, 11**). This upper section transitions southward to laterally extensive

FIGURE 5 | Chingue slope unit stratigraphic architecture and facies.
(A) Southward view of El Chingue Bluff (location 5A, **Figures 2C**, **3**)
characterized by thin and thick bedded non-amalgamated turbidites (F4 and
F5) within both the hanging wall and foot wall of a synthetic growth fault
(indicated by white arrowheads); clastic intrusions are parallel or sub-parallel
to the faults (cf. Shultz and Hubbard, 2005). **(B)** Interbedded mudstone (F1)
and tabular non-amalgamated sandstone (F4), with lenticular scour-fill also
present (F5) (base demarcated by thin dashed white line). Note person
(circled) for scale. **(C)** Chaotically bedded fine-grained sandstone and
mudstone deposits (F2) overlain by interbedded mudstone (F1) and
sandstone (F4 and F5) (separated by white dashed line). The overlying facies
are interpreted to have infilled rugose topography on top of the chaotically
bedded deposits. **(D)** Slumped deposits (F2) encased in concordant
mudstone (F1). The base and top of the slumped deposits are indicated with
white arrowheads. Person at lower right for scale. All outcrop locations are
denoted by Figure number within **Figures 2C**, **3**.

(km-scale), upward-coarsening and bed-thickening packages 20–
60 m thick composed of interbedded fine-grained sandstone and
mudstone (Facies F1, F4) (**Figures 10F,G**, **11**). The most distal
deposits at the base, which make up most of the thickness of
this unit, are primarily fine grained (Facies F1), punctuated by

thin and lenticular sandstone-filled channel forms characterized
by variably oriented stratification, including backsets (Facies
F5-F6) (**Figures 10D,E** and **Table 1**). Notably, the upper
half of this unit is exceptionally exposed along a series of
unvegetated mountainside outcrops, which display seismic-
scale stratal geometries characterized by basinward-dipping
and basinward-thinning packages overlain by flatter units (i.e.,
apparent toplap) (**Figures 10A**, **11**). Collectively, these strata
record the progradation of Oveja shelf-margin clinoforms.

We interpret the sharp lithologic change from deltaic
sandstone of the upper Figueroa clinothem to overlying
mudstone of the basal Oveja clinothem to reflect a backstep of
the shelf (**Figure 8**; Houseknecht and Shank, 2004; Henriksen
et al., 2011). The emplacement of distal slope facies on the
proximal deltaic deposits (**Figures 3**, **4**, **10A–C**) indicates a
landward shift of facies above the Figueroa clinothem. The
magnitude of apparent backstep (i.e., > 10 km) and landward shift
of facies could represent a basin-wide event and reorganization
of the shelf-slope system (**Figure 1C**; cf. Ross et al., 1994).
Although the 3-D character of shelf-margin migration and its
driving mechanism are speculative, orogenic activity in the
adjacent Andean Cordillera and associated basin subsidence and
transgression of the shoreline could have influenced stratigraphic
sequence development (cf. Cant and Stockmal, 1989; Laskowski
et al., 2013). Correlation between events in the fold-and-thrust
belt (Fosdick et al., 2011) and the timing of this major landward
retreat of facies cannot be constrained with current data.
However, Daniels et al. (2018) showed that this transgression took
place at ∼75 Ma, which corresponds to a time of significant global
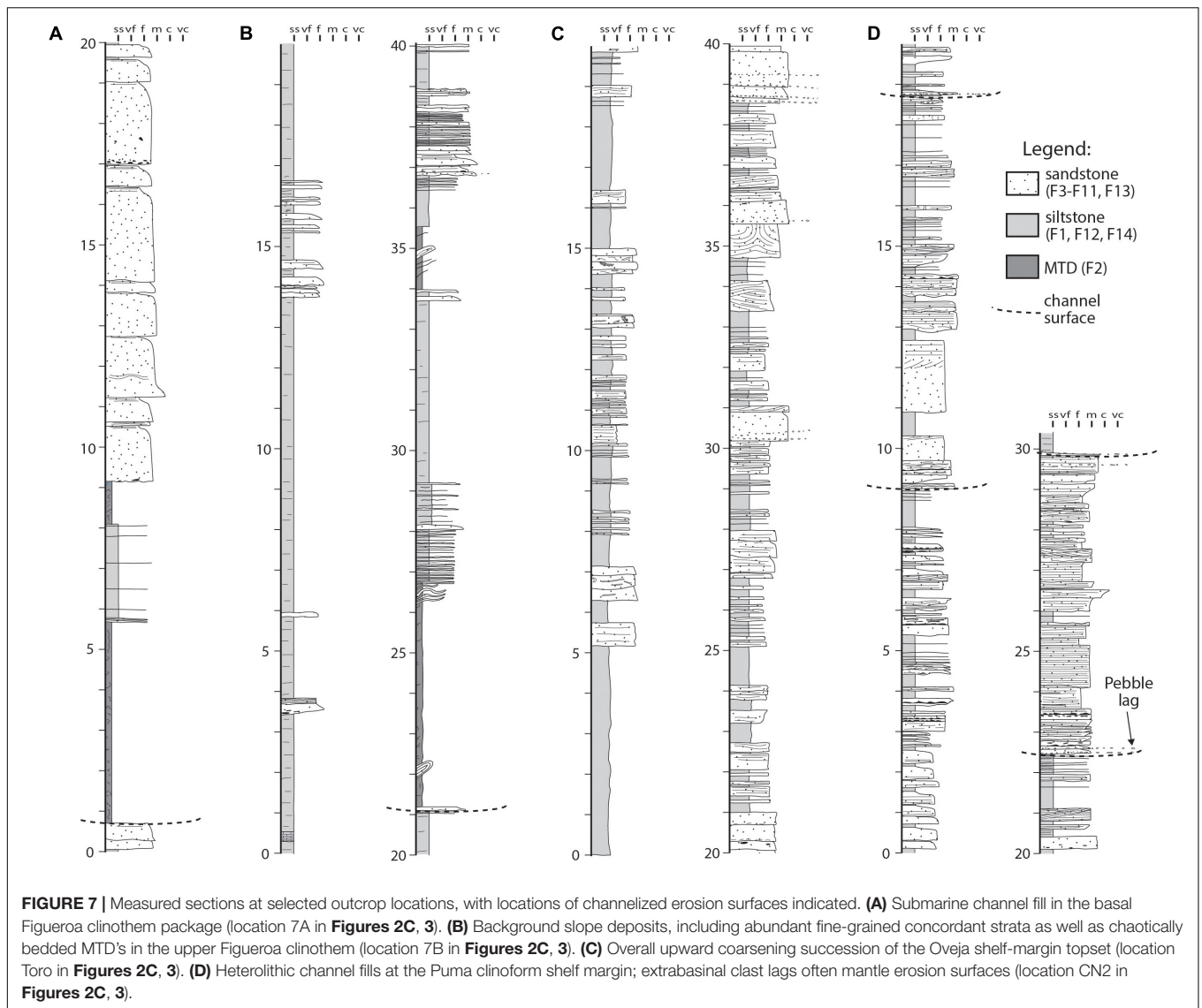sea-level rise (Kominz et al., 2008).

We interpret that sustained sediment supply promoted
progradation of the Oveja basin margin at Cerro Cazador
(**Figures 8**, **11**). The 300–400 m-relief clinoforms prograded
toward the abandoned, or relict shelf edge break-in-slope
of the underlying high-relief Figueroa shelf-margin unit
(**Figure 8E**). Regardless of potential external (e.g., Carvajal
et al., 2009) or internal (e.g., Gerber et al., 2008) drivers on
the accommodation/supply regime, as the relict shelf edge was
encountered, a period of slope instability and failure (i.e., out-of-
grade conditions) led to truncation of the Oveja clinothem topset
and initiation of the Puma shelf-margin unit (**Figure 8F**).

The Puma Shelf-Margin Unit

The basal 20–100 m thick Puma basal clinothem package
(**Figure 3**) is correlated for 35–40 km along paleoslope (**Figure 4**).
In the most proximal location on Cerro Cazador (**Figures 11B**,
12), sandstone-dominated strata (Facies F8, F10, F13) overlie
undulatory surfaces with up to 4 m of relief. Basinward, upward-
coarsening packages (F8, F10-F11, F13–14) are truncated by
multiple concave-up surfaces with 5–60 m relief that are up
to 150 m wide (minimum estimate based on partial strike
view; **Figures 12**, **13A–D**). These surfaces define channel
forms composed of mostly heterolithic deposits (F14) including
lenticular sandstone beds with rare pebble lags (F7) (**Figures 7D**,
13C). More distally, the basal Puma clinothem package largely
comprises fine-grained deposits (F11, F13, F14) that are truncated
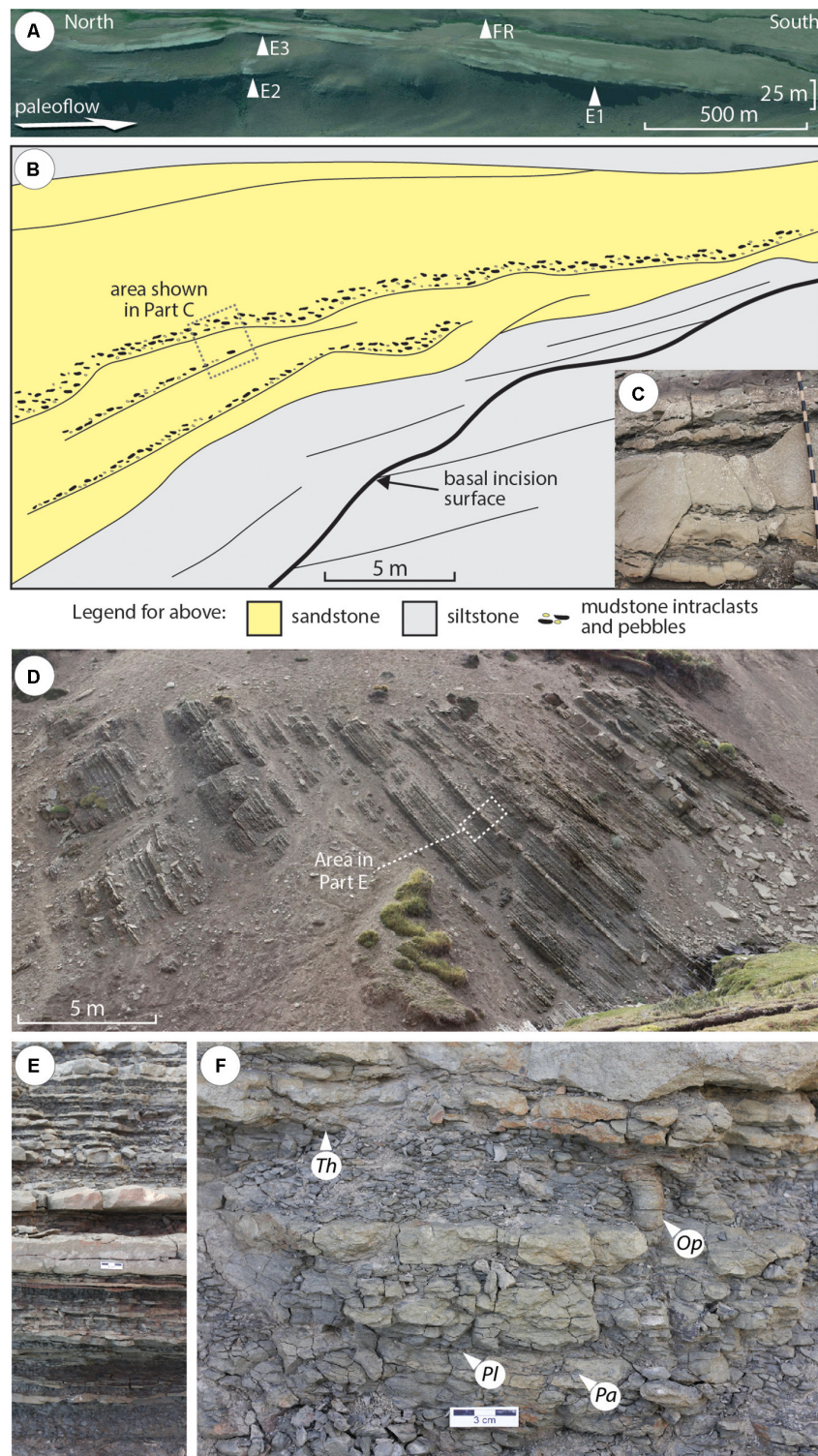
FIGURE 6 | Figueroa shelf-margin stratigraphic architecture and facies. **(A)** Depositional dip-oriented perspective satellite image featuring discontinuously resistant, along-slope channel sandstone deposits (white arrows; locations E1-E3 and FR in **Figures 2C**, **3**) (image data from Google, Landsat, Copernicus, 2016, http://google.com/earth/index.html). **(B)** Outcrop sketch of channel fill with the basal incision surface draped by mudstone-dominated turbidites, and subsequently overlain by amalgamated thick-bedded sandstone deposits (F3). **(C)** Variably amalgamated thick- to thin-bedded turbidites with common mudstone clasts; Jacob staff is 1.5 m in length. **(D)** Interbedded tabular, normally graded sandstone (F4) and carbonaceous mudstone (F1). **(E)** Interbedded tabular normally graded fine- to medium-grained sandstone (F4) and mudstone (F1) [location in **(D)**]. Scale bar in middle of photo is 3 cm long. **(F)** Bioturbated mudstone (F1) and fine- to medium-grained sandstone (F4) with rare *Thalassinoides* (Th), *Ophiomorpha* (Op), *Palaeophycus* (Pa) and *Planolites* (Pl). All outcrop locations are denoted by Figure number in **Figures 2C**, **3**.

FIGURE 7 | Measured sections at selected outcrop locations, with locations of channelized erosion surfaces indicated. **(A)** Submarine channel fill in the basal Figueroa clinothem package (location 7A in **Figures 2C**, **3**). **(B)** Background slope deposits, including abundant fine-grained concordant strata as well as chaotically bedded MTD's in the upper Figueroa clinothem (location 7B in **Figures 2C**, **3**). **(C)** Overall upward coarsening succession of the Oveja shelf-margin topset (location Toro in **Figures 2C**, **3**). **(D)** Heterolithic channel fills at the Puma clinoform shelf margin; extrabasinal clast lags often mantle erosion surfaces (location CN2 in **Figures 2C**, **3**).

by concave surfaces with 1–5 m relief, which are overlain by similar interbedded facies (**Figures 13E,F**).

Evidence for mass wasting and slump-induced concave-up surfaces at the shelf margin at Cerro Cazador (**Figures 13A–D**) mark the position of the Puma shelf edge (**Figure 8**). As the Oveja basin margin prograded to the abandoned, relict shelf edge of the underlying Figueroa shelf margin unit (**Figure 8**), the shelf-margin relief increased and a period of slope readjustment ensued (**Figure 8E**). Regional mapping shows that just basinward of the associated shelf-edge delta, the paleoslope was at its steepest (**Figure 4**). The Puma margin records a basinward shift of facies and the introduction of abundant sand and gravel into the basin (e.g., Plink-Björklund and Steel, 2005; Houseknecht et al., 2009). Reimchen et al. (2016) demonstrated that 35 km basinward from the mapped shelf margin on Cerro Cazador, the Puma basal clinothem package is composed of conglomerate- and sandstone-dominated submarine channel deposits >60 m thick (**Figure 4**). After a period of enhanced coarse-grained sediment delivery to

deep water, deposition of mudstone-prone slope facies ensued as the shelf-edge trajectory began to rise sharply (**Figure 4**). Slope strata are largely dominated by mudstone above the Puma clinoform across the Cerro Cazador study area.

The Stratigraphic Record of Sediment Transfer Along High-Relief Clinoforms

The outcropping stratigraphic record at Cerro Cazador shows evidence of net-depositional slope processes, including voluminous fine-grained strata that compose the Chingue unit, and the Figueroa, Oveja and Puma shelf-margin units (**Figure 4**). We interpret that a significant proportion of the slope strata is a result of hemipelagic or channel-overbank sedimentation of fine-grained material (Normark et al., 1993; Deptuck et al., 2003; Kane and Hodgson, 2011; Poyatos-Moré et al., 2016).

Shelf-edge to upper-slope conduit development directly overlying the Puma clinoform on Cerro Cazador, including

FIGURE 8 | Simplified depositional evolution of shelf-margin strata in the Magallanes Basin study area (from **Figure 4**). Part **(A)** is the first evolutionary stage through to part **(G)**, which is the last. Although at this scale clinoforms can only be drawn in a way that implies fairly straightforward correlation of simple surfaces over tens of kilometers, the results of detailed sedimentological and stratigraphic architecture analysis indicate that these surfaces are typically composite features that formed over a protracted period

(Continued)

FIGURE 8 | Continued

in many instances. In parts **(C,G)**, enhanced sediment bypass of the upper slope and sand/gravel deposition in the basin was facilitated. Red dots indicate approximate locations of features figured in the manuscript: 1 (**Figures 5A,B**); 2 (**Figures 5C,D**); 3 (**Figures 6A, 14B**); 4 (**Figures 6B, 7A**); 5 (**Figures 9B–D**); 6 (**Figures 7B, 9A**); 7 (**Figures 10D,E**); 8 (**Figures 7C, 11**); 9 (**Figures 7D, 13A–D**); 10 (**Figure 13E**). Note that PPC = the confluence of the Puma Clinoform and Arroyo Picana.
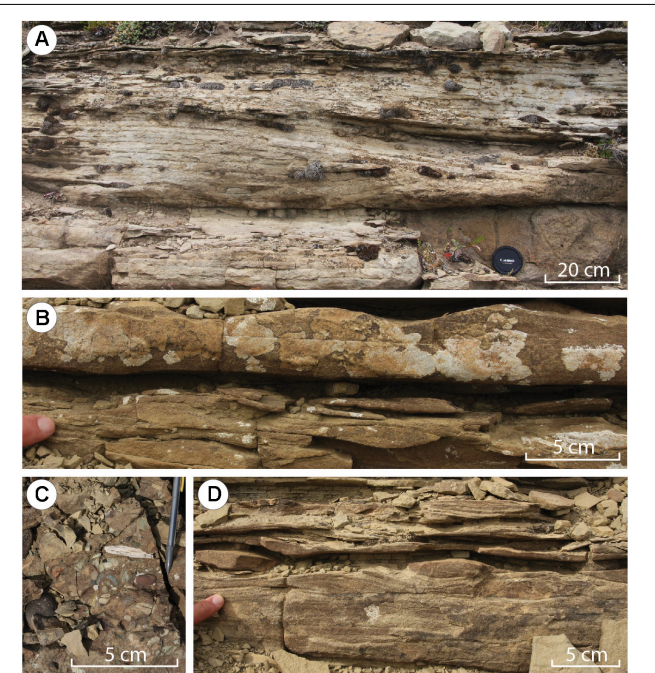
FIGURE 9 | Figueroa basin margin topset facies. **(A)** Hummocky cross-stratified (HCS) fine-grained sandstone (F9). **(B)** Symmetrical (top) and asymmetrical ripples (below) within fine-grained sandstone deposits (F9). **(C)** Coarse-grained sandstone with pebbles, granules, shell material, and woody debris (F7). **(D)** Planar laminae overlain by asymmetrical ripples in fine-grained sandstone deposits (F13). All outcrop locations are denoted by figure number within **Figures 2C,E**, **3**.

mass-wasting deposits overlain by channel forms up to 60 m thick, records initiation of a zone of predominantly coarse-grained sediment bypass (**Figures 13A–D**; cf. Nemec et al., 1988; Anderson et al., 1996; Jones et al., 2013). The channel fills are largely dominated by heterolithic thin- to thick-bedded strata with very thin sandstone and pebble lags that are among the coarsest deposits on the slope (**Figure 7D**). Such features are interpreted to provide a template for channelized sediment transfer to deep water (Mayall et al., 1992; Porebski and Steel, 2003; Ridente et al., 2007; Sylvester et al., 2012; Gomis-Cartesio et al., 2018; Gales et al., 2019).

Extensive tracts of basal clinothem packages, between the shelf edge and lower slope, are characterized by abundant cross-cutting erosional surfaces with >10 m of relief, as well as the complex superposition of channel fills, mass-wasting deposits, ponded sandstones and lag deposits (**Figure 14**). Collectively, these deposits highlight the protracted development of stratigraphic
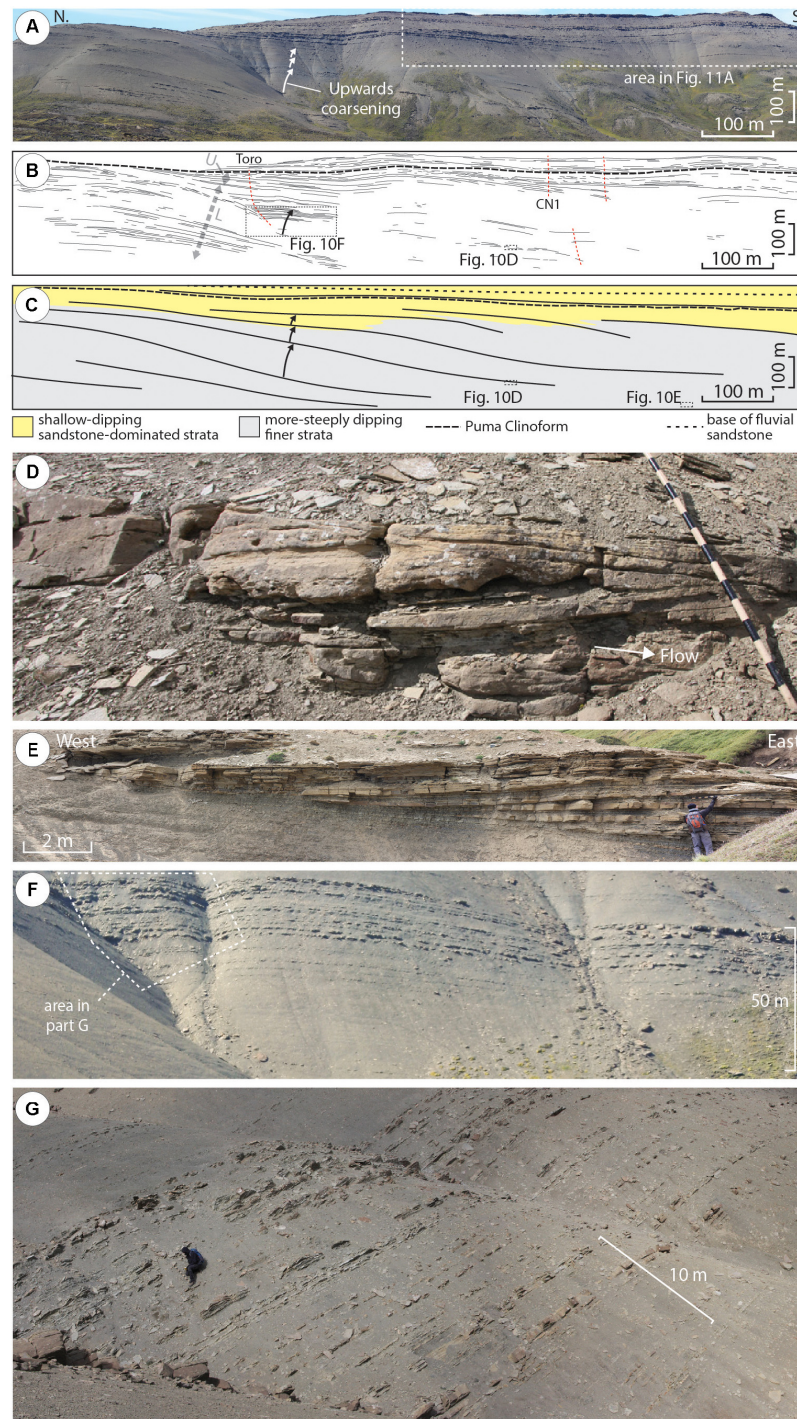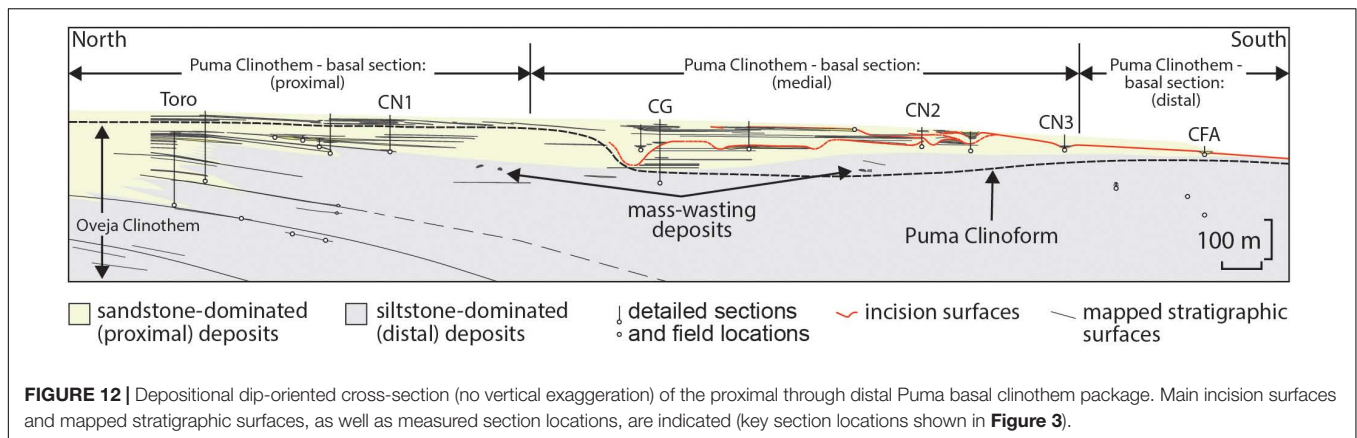
FIGURE 10 | Oveja shelf-margin stratigraphic architecture and facies. **(A)** Depositional dip perspective with an emphasis on coarsening upward packages (white arrows); the top of the section is dominated by sandy deposits (see **Figure 2E** for location). **(B)** Line-drawing trace of **(A)**, which enhances stratigraphic surfaces, including relatively shallow dipping topset strata (top of image) and more steeply dipping slope strata (middle to base of image). Gray dashed line approximates the boundary between lower (L), and upper (U) sections of the clinothem, as described. The black dashed black line demarcates the Puma clinoform. Selected measured section locations are shown with sub-vertical dashed red lines. **(C)** Schematic diagram showing the interpretation of stratigraphic architecture in **(A,B)**. **(D)** Non-amalgamated cross-bedded medium-grained sandstone (F6) within lenticular channel form [location shown on **(C)**]. Variably oriented cross-stratification, including backsets, suggest that these bodies formed during phases of high discharge (Ponce and Carmona, 2011; Hage et al., 2018). **(E)** Semi- to non-amalgamated wedge, in which the beds lap out or pinch out at the basal to marginal edge of a lenticular sedimentary body [location shown on Part **(C)**]. **(F)** Overall coarsening upward package [location shown on **(B)**]. **(G)** Interbedded normally graded planar-laminated sandstone (F13) and carbonaceous mudstone (F1) toward the top of a thick upward-coarsening section.

FIGURE 11 | (A) Photo-mosaic and **(B)** line-drawing trace of the upper portion of the Oveja shelf margin and the proximal deposits overlying the Puma clinoform showing river dominated deltaic clinoforms dipping basinward and transitioning into siltstone-dominated slope deposits. See **Figure 10A** for location. **(C)** Photo mosaic of deltaic clinoform topset highlighted in **(A)**. **(D–F)** Facies of the upper section of the Oveja clinothem, including: **(D)** Detailed stratigraphic section of typical sandstone-dominated coarsening upward package with interbedded carbonaceous mudstone (F14) and thin-bedded sandstone (F13) overlain by planar-laminated sandstone (F8) and coarse- to very coarse-grained lenticular sandstone (F7). Section location is shown in **(C)**. **(E)** Loading structure in medium-grained sandstone (F10); Jacob staff at base of photo is 1.5 m long (outcrop location is top of Toro section; **Figure 3**). See bed in measured section (**Figure 7C**) at 35 m for stratigraphic context. **(F)** Planar and trough cross-stratified medium-grained sandstone (F7); 10 cm intervals indicated on Jacob staff. Location is section CN (**Figure 3**).

surfaces in response to a variety of processes including erosion, sediment bypass, mass-wasting and deposition from gravity flows (Hodgson et al., 2016). Bed-scale evidence for high-energy currents that bypassed a portion of their sediment load along the basal sections of the Figueroa and Puma clinothems include: (1) conglomeratic lag deposits; (2) cross bedding; and (3) mudstone drapes that mantle erosion surfaces, which are interpreted to record deposition from the tails of largely bypassing turbidity currents (**Table 1**; cf. Mutti and Normark, 1987; Stevenson et al., 2015). Sedimentary body-scale evidence

for prolonged sediment transfer across the Magallanes Basin slopes are represented by mass-wasting deposits (F2) including large rafted sediment blocks (**Figure 13B**), channel forms with evidence for a polyphase history of multiple cut-and-fill events (5–20 m thick) (**Figures 6A–C**, **7A**), and channel forms filled primarily with thinly interbedded turbidites (**Figures 13E,F**; cf. Hubbard et al., 2014; Stevenson et al., 2015).

Perhaps the most significant record of sediment bypass along the Figueroa and Puma basal clinothem packages in the Cerro Cazador study area is the increase in overall proportion of

FIGURE 12 | Depositional dip-oriented cross-section (no vertical exaggeration) of the proximal through distal Puma basal clinothem package. Main incision surfaces and mapped stratigraphic surfaces, as well as measured section locations, are indicated (key section locations shown in **Figure 3**).

sandstone and conglomerate deposits from upper slope strata downslope 30–40 km to the south, in the vicinity of Arroyo Picana and Laguna Figueroa (**Figures 4**, **8**; Macauley and Hubbard, 2013; Hubbard et al., 2014; Pemberton et al., 2016; Reimchen et al., 2016). Coarse-grained lower-slope to basin-floor deposits are commonly linked to laterally extensive (kilometers), deep (10's of meters) incisions and canyons developed along the coeval shelf margin (e.g., Anderson et al., 1996; Johannessen and Steel, 2005; Ryan M. C. et al., 2009; Henriksen et al., 2011; Sylvester et al., 2012).

DISCUSSION: DEPOSITIONAL TOPOGRAPHY CONTROL ON SLOPE READJUSTMENT

The Campanian shelf-margin to slope depositional system at Cerro Cazador is dominated by mudstone across the 2-2.5 km thick and >60 km long transect (**Figures 2F**, **4**). Two prominent sandstone-rich packages mantle clinoform surfaces (i.e., Figueroa and Puma basal clinothem packages), standing out amongst the fine-grained stratigraphic backdrop. As such, they represent an opportunity to investigate the topographic controls on coarse-grained sediment delivery across a high-relief basin margin in the context of well-defined stratigraphic architecture, sediment-routing history, and source-area evolution (Romans et al., 2010, 2011; Fosdick et al., 2011; Bernhardt et al., 2012; Daniels et al., 2018).

We document ∼8 Myr of coarse-grained sediment transfer beyond the shelf margin in the deep-water Magallanes Basin (Daniels et al., 2019). Ross et al. (1994) proposed a series of mechanisms associated with shelf-margin readjustment that lead to enhanced coarse-grained sediment delivery beyond the shelf margin (**Figure 1**); however, the predicted stratigraphic architecture has yet to be widely linked to an outcrop record.

At Cerro Cazador, an early phase of instability is recorded by the Chingue unit, which comprises growth faults, extensive sandstone intrusions, and chaotically bedded deposits indicative of unstable slope conditions (**Figures 4**, **5**). These strata accumulated over 2-2.5 Myr and are mapped beyond the study area for up to 100 km north-south along depositional

dip (Daniels et al., 2018). The extensive period of mass wasting resulted in a southward-thinning wedge of dominantly MTDs up to 900 m thick at Cerro Cazador, where it then thins to <500 m southward over a distance of only ∼20 km. We speculate that the thickest composite slope sandstone accumulation (∼300 m) in the basin resulted from progradation of the Figueroa basin margin to the break-in-slope at the top of the Chingue interval where MTDs begin to thin rapidly to the south (**Figure 8**). This observed change in basin margin architecture associated with prominent antecedent topography combined with the introduction of voluminous sand and gravel to the basin is consistent with the interpretation that the clinoform slope oversteepened, initiating the long-lived (up to >2 Myr; Daniels et al., 2018) Figueora channel system. Up slope, the Figueroa system is characterized by substantial erosion and sediment bypass, which transitions down slope to hundreds of meters of submarine channel strata that is comparable to channel deposits in continental margin strata (Macauley and Hubbard, 2013; Fowler and Novakovic, 2018; Pemberton et al., 2018; Jackson et al., 2019). The generation of this oversteepened slope is similar to a mechanism proposed by Ross et al. (1994), wherein steep slopes develop as a result of fluctuating carbonate and siliciclastic deposition and/or tectonic deformation. In mixed siliciclastic and carbonate systems, following carbonate platform development, deltas reach the relict carbonate platform edge and the oversteepened slope leads to prolonged coarse-grained sediment delivery to deep water (see Scenario B; **Figure 1C**). Using a modeling approach, Uličný et al. (2002) showed that 2-D stacking patterns of shelf-slope-basin clinoform systems are highly sensitive to initial depth (i.e., water depth at onset of deposition). Their study focused on tectonic (fault) inheritance whereas we emphasize topography inherited from the previous depositional phase. In the Chilean basin, instead of development of a break in slope at a relict carbonate platform edge, a morphologically similar scenario was established through the emplacement of mass-transport deposits prior to development of the Figueroa shelf-margin (**Figure 8A**).

The large-magnitude backstep on top of the Figueroa basin margin set the stage for an additional, protracted phase of slope instability and submarine-fan development
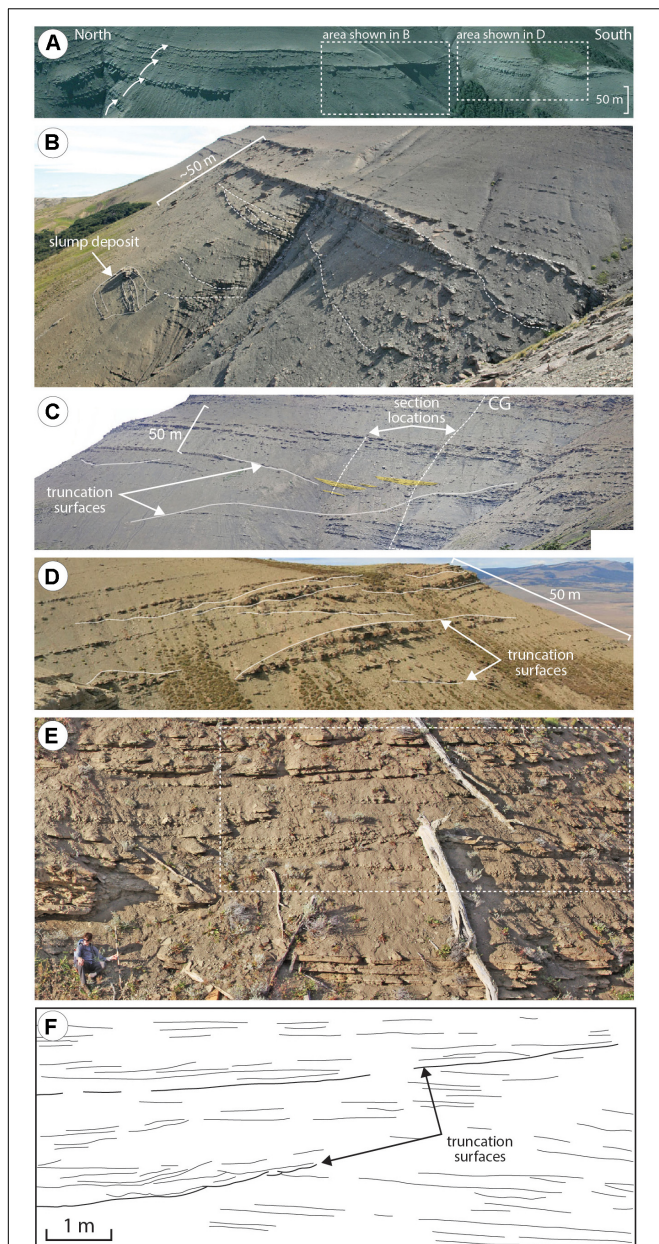
FIGURE 13 | Puma basal clinothem package stratigraphic architecture and facies. **(A)** Dip-oriented satellite image of Cerro Cazador near the interpreted Puma clinoform shelf margin (refer to **Figure 2E** for location). White arrows highlight coarsening upward packages (image data: Google, Landsat, Copernicus, 2016, http://google.com/earth/index.html). **(B)** Incision surfaces (dashed white lines) cutting deltaic strata at the shelf margin. Location shown in **(A)**. **(C)** Strike perspective of a significant incision surface (lowest example), which truncates interbedded mudstone and sandstone, and is infilled with comparable facies as well as channelized sandstone (yellow). Paleoflow is approximately out of the page; sub-vertical white lines indicate the location of measured sections (**Figure 2E** for location). **(D)** Multiple erosion surfaces (white lines) that truncate deltaic deposits in proximity to the shelf edge rollover. Location shown in **(A)**. **(E)** Photograph and **(F)** line drawing trace of fine-grained sandstone and mudstone at a distal location of the Puma basal clinothem package. Truncation surfaces are apparent, and erosional relief is in-filled with facies similar to that which was incised. Outcrop location denoted on **Figures 2C,E**, **3**.
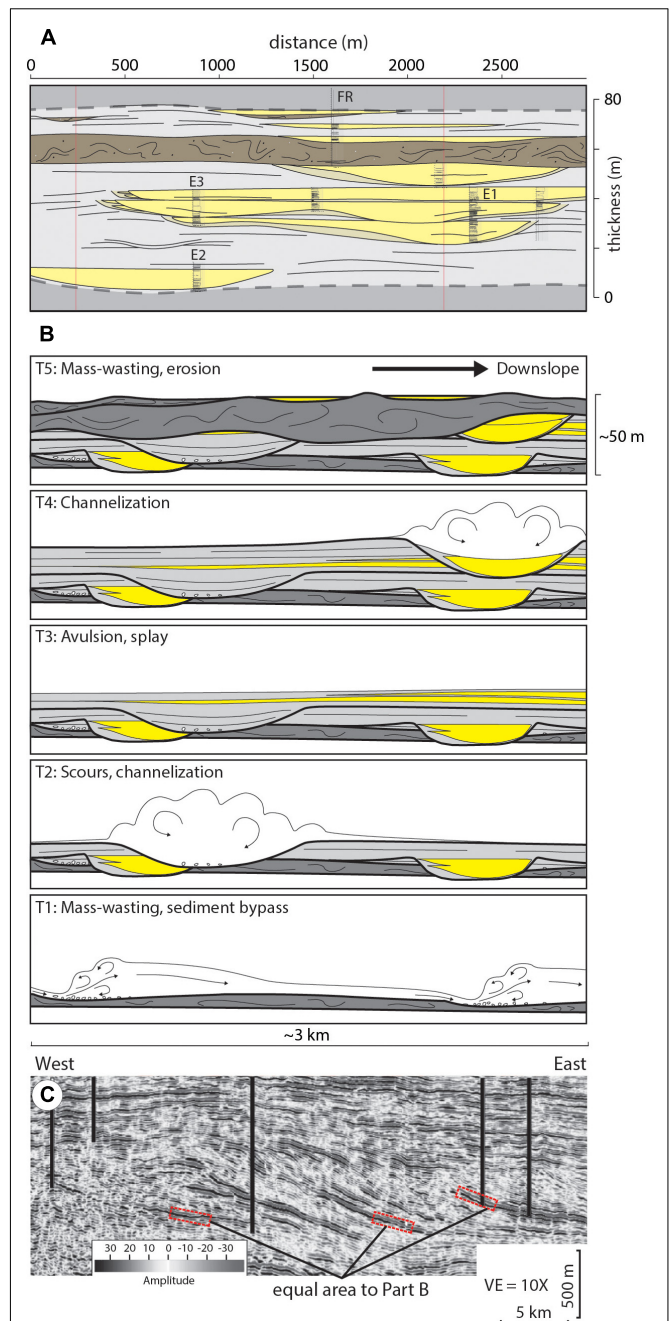
FIGURE 14 | (A) Dip-oriented schematic cross-section of channelized strata that compose a segment of the basal Figueroa clinothem package (see **Figure 6A** for outcrop overview). A similarly scaled perspective to this section is presented at various locations in **(C)** (red outlined boxes). **(B)** Schematic evolution of the sandstone-prone basal clinoform package in **(A)**. The area featured is comparable in scale and character to that featured in **(A)**. A sustained period of elevated off-shelf coarse-grained sediment transfer results in a composite sedimentary package defined by deposits that record erosion, mass-wasting, sediment bypass and deposition. **(C)** Vertical seismic section from the Magallanes Basin highlighting prograding clinothems up to 600–800 m thick, providing context for the basal clinothem segment featured in **(A)** (modified from Gallardo, 2014). The Late Eocene-Early Miocene strata record the infilling of the deep-water basin approximately 150 km south of the Cerro Cazador study area along the foreland basin axis.

(**Figure 8E**). This backstep is followed by the progradation of the Oveja basin margin to the abandoned, relict shelf edge of the Figueroa basin margin. The corresponding change in shelf-margin physiography led to a period of oversteepening that resulted in erosion of Oveja shelf-margin strata and initiation of the coarse-grained basal Puma clinoform package (**Figures 8F,G**). Similar to Figueroa strata, submarine-channel systems that are compositionally and architecturally similar to examples documented from continental margins are mapped along the system (Reimchen et al., 2016). The observed stratigraphic architecture at Cerro Cazador is consistent with scenario A of Ross et al. (1994), as shown in **Figure 1C**.

The erosional Figueroa and Puma clinoforms mark the disruption of a graded shelf-margin profile (**Figure 4**). Antecedent topography inherited from preceding phases significantly influenced the development of subsequent shelf margins including oversteepened upper slopes, and the transfer of coarse-grained sediment to deep water. Whether the inherited topography was a result of initial configuration (e.g., tectonic) or from predecessor clinoform shelf-margin position, the break in the slope profile caused the system to reach a disequilibrium state.

An important goal of sedimentary geoscientists is to gain insights into the controls on sedimentation and the creation of the depositional record for prediction in analogous settings. In an effort to communicate to colleagues and the broader geoscience community, we commonly attempt to place our interpretations in the context of allogenic versus autogenic controls (e.g., Beerbower, 1964; Paola et al., 2009). Allogenic controls are external to the sediment-routing and depositional system, including changes in eustatic sea level, tectonics, climate, and initial geometry of the receiving basin, whereas autogenic controls are internal to the sedimentary system, including intermittent sediment storage producing episodic, spatially discontinuous sedimentation (Romans et al., 2016; Hajek and Straub, 2017) and landward retreat of deltaic prisms in response to changing area and slope during deposition (Muto and Steel, 2002). However, some controls do not clearly fit into an either/or, allogenic/autogenic dichotomy. The disruption of graded shelf-margin profiles in response to inherited depositional topography during basin evolution is one such control. For example, although receiving-basin geometry can be considered an allogenic control governed by underlying tectonic configuration (Nelson and Kulm, 1973; Mutti and Normark, 1987), subsequent basin filling creates the depositional topography across which sediment transport and deposition occur to create stratigraphic architecture (e.g., Burgess et al., 2008). In this way, both external tectonic underpinning and internal dynamics of sedimentation govern resultant topography, which, in turn, influences the occurrence and position of shelf margins prone to deliver coarse sediment to the basin. Beyond understanding controls on margin evolution through major slope readjustments, there are implications for reservoir prediction associated with hydrocarbon exploration or carbon storage (see Ross et al., 1994); for example, the thickest, coarsest turbidite accumulations onlap erosional shelf-margin clinoforms and develop downstream of paleotopographic escarpments (**Figures 8C,G**). Additionally, with sufficient data coverage (outcrop or subsurface) the prediction of stacking patterns and facies in the context of inherited topography has the advantage of such features being potentially preserved and identified in the physical stratigraphic record without invoking assumptions about external forcings that are difficult or, in some cases, impossible to constrain.

CONCLUSION

A large-scale shelf-to-slope depositional system featuring basin margins with >1000 m paleobathymetric relief and slope lengths >40 km is preserved in outcropping Cretaceous strata of Chilean Patagonia. The depositional architecture observed in these outcrops is analogous to seismically imaged clinoforms of slope systems worldwide. The strata are characterized by evidence for the development of two key coarse-grained sediment-delivery systems that resulted in fairways of sandstone-dominated submarine-channel deposits >100 m thick in the deep-water basin: the Figueroa and Puma clinoforms. The stratigraphic position and architecture of each leads to an interpretation that they formed during major slope readjustments, across initially oversteepened depositional topography, which resulted in transient out-of-grade slope conditions. Strata directly overlying the Figueroa and Puma clinoforms (i.e., basal clinothem packages) are sandstone-rich, recording phases of enhanced coarse-grained sediment delivery to the deep-water basin. The 35 km long and up to 2.5 km thick stratigraphic section represented by the two slope systems was largely associated with mudstone, deposited over 3–4 Ma. The only two large-scale sandstone accumulations in the 2-D outcrop belt are recorded by the Figueroa and Puma basal clinothem packages, demonstrating the importance of major slope readjustments in margin evolution. Pre-existing depositional topography controls the locations of subsequent shelf margins and coarse-grained sediment delivery to deep water. Understanding this control has predictive value in analogous settings that were subjected to intermittent oversteepening and transient phases of coarse-grained sediment bypass to deep water.

DATA AVAILABILITY STATEMENT

All datasets generated for this study are included in the article/supplementary material.

AUTHOR CONTRIBUTIONS

DB did the fieldwork as a graduate student and wrote the initial draft. SH envisioned the project, secured the funding, assisted with fieldwork, and edited the manuscript. JC and BR assisted in the field and with manuscript preparation, including formulating the purpose, and organization of the manuscript.

REFERENCES

Adeogba, A., McHargue, T. R., and Graham, S. A. (2005). Transient fan architecture and depositional controls from near-surface 3-D seismic data, Niger Delta continental slope. *AAPG Bull.* 89, 627–643. doi: 10.1306/11200404025

Anderson, J. B., Abdulah, K., and Sazalejo, S. (1996). "Late quaternary sedimentation and high-resolution sequence stratigraphy of the east Texas shelf," in *Geology of Siliciclastic Shelf Seas*, eds M. de Batist, and P. Jacobs, (London: Geol. Soc. Special Publication), 95–124. doi: 10.1144/gsl.sp.1996.117.01.06

Arbe, H. A., and Hechem, J. J. (1984). Estratigrafi'a y facies de depo'sitos marinos profundos del Creta'cico Superior, Lago Argentino, Provincia de Santa Cruz (Stratigraphy and deep marine deposition facies of the Upper Cretaceous, Lago Argentino, Santa Cruz). *Congreso Geologico Argentino* 9, 7–41.

Armitage, D. A., Romans, B. W., Covault, J. A., and Graham, S. A. (2009). The influence of mass-transport deposit surface topography on the evolution of turbidite architecture: the sierra contreras, tres pasos formation (Cretaceous), southern Chile. *J. Sed. Res.* 79, 287–301. doi: 10.2110/jsr.2009.035

Auchter, N. C., Romans, B. W., and Hubbard, S. M. (2016). Influence of deposit architecture on intrastratal deformation, slope deposits of the Tres Pasos Formation. *Chile. Sed. Geol.* 341, 13–26. doi: 10.1016/j.sedgeo.2016.05.005

Bauer, D. B. (2012). *Stratigraphic Evolution of a High-Relief Slope Clinoform System, Magallanes Basin, Chilean Patagonia.* M.Sc. Thesis, University of Calgary, Calgary.

Beerbower, J. R. (1964). Cyclothem and cyclic depositional mechanisms in alluvial plain sedimentation. *Kansas Geol. Surv. Bull.* 169, 31–42.

Bernhardt, A., Jobe, J. R., Grove, M., and Lowe, D. R. (2012). Palaeogeography and diachronous infill of an ancient deep-marine foreland basin, Upper Cretaceous Cerro Toro Formation, Magallanes Basin. *Basin Res.* 24, 269–294. doi: 10.1111/j.1365-2117.2011.00528.x

Burbank, D. W. (1992). Causes of recent Himalayan uplift deduced from deposited patterns in the Ganges basin. *Nature* 357, 680–683. doi: 10.1038/357680a0

Burgess, P. M., Steel, R. J., and Granjeon, D. (2008). "Stratigraphic forward modeling of basin-margin clinooform systems: implications for controls on topset and shelf width and timing of formation of shelf-edge deltas," in *Recent Advances in Models of Siliciclastic Shallow-Marine Stratigraphy*, Vol. 90, eds G. J. Hampson, R. J. Steel, P. M. Burgess, and R. W. Dalrymple (Tulsa: Society for Sedimentary Geology Special Publication), 35–45.

Cant, D. J., and Stockmal, G. S. (1989). The Alberta foreland basin: relationship between stratigraphy and Cordilleran terrane-accretion events. *Can. J. Earth Sci.* 26, 1964–1975. doi: 10.1139/e89-166

Carvajal, C., Steel, R., and Petter, A. (2009). Sediment supply: the main driver of shelf-margin growth. *Earth Sci. Rev.* 79, 221–248. doi: 10.1016/j.earscirev.2009.06.008

Carvajal, C. R., and Steel, R. J. (2009). Shelf-edge architecture and bypass of sand to deep water: influence of shelf-edge processes, sea level, and sediment supply. *J. Sed. Res.* 79, 652–672. doi: 10.2110/jsr.2009.074

Cosgrove, G. I. E., Hodgson, D. M., Poyatos-More, M., Mountney, N. P., and McCaffrey, W. D. (2018). Filter or conveyor? Establishing relationships between clinoform rollover trajectory, sedimentary process regime, and grain character within intrashelf clinothems, Offshore New Jersey, U.S.A. *J. Sed. Res.* 88, 917–941. doi: 10.2110/jsr.2018.44

Covault, J. A., Romans, B. W., and Graham, S. A. (2009). Outcrop expression of a continental-margin shelf-edge delta from the Cretaceous Magallanes Basin. *Chile. J. Sed. Res.* 79, 523–539. doi: 10.2110/jsr.2009.053

Crane, W. H., and Lowe, D. R. (2008). Architecture and evolution of the Paine channel complex, Cerro Toro Formation (Upper Cretaceous), Silla Syncline, Magallanes Basin, Chile. *Sedimentology* 55, 979–1009. doi: 10.1111/j.1365-3091.2007.00933.x

Dalziel, I. W. D. (1981). Back-arc extension in the southern andes: a review and critical reappraisal. *Roy. Soc. Lon. Philosoph. Trans. ser. A* 300, 319–335. doi: 10.1098/rsta.1981.0067

Daniels, B. G., Auchter, N. C., Hubbard, S. M., Romans, B. W., Matthews, W. A., and Stright, L. (2018). Timing of deep-water slope evolution constrained by large-n detrital zircon and volcanic ash geochronology, Cretaceous Magallanes Basin, Chile. *Bull. Geol. Soc. Am.* 130, 438–454. doi: 10.1130/b31757.1

Daniels, B. G., Hubbard, S. M., Romans, B. W., Malkowski, M. A., Matthews, W. A., Bernhardt, A., et al. (2019). Revised chronostratigraphic framework for the Cretaceous Magallanes-Austral Basin, Ultima Esperanza Province, Chile. *J. South. Am. Earth Sci.* 94:102209. doi: 10.1016/j.jsames.2019.05.025

Deptuck, M. E., Steffens, G. S., Barton, M., and Pirmez, C. (2003). Architecture and evoltion of upper fan channel-belts on the Niger Delta slope and in the Arabian Sea. *Mar. Pet. Geol.* 20, 649–676. doi: 10.1016/j.marpetgeo.2003.01.004

Dixon, J. F., Steel, R. J., and Olariu, C. (2012a). River-dominated, shelf-edge deltas: delivery of sand across the shelf break in the absence of slope incision. *Sedimentology* 59, 1133–1157. doi: 10.1111/j.1365-3091.2011.01298.x

Dixon, J. F., Steel, R. J., and Olariu, C. (2012b). Shelf-edge delta regime as a predictor of deep-water deposition. *J. Sed. Res.* 82, 681–687. doi: 10.2110/jsr.2012.59

Driscoll, N. W., and Karner, G. D. (1999). Three-dimensional quantitative modeling of clinoform development. *Mar. Geol.* 154, 383–398. doi: 10.1016/s0025-3227(98)00125-x

Fildani, A., Cope, T. D., Graham, S. A., and Wooden, J. L. (2003). Initiation of the Magallanes foreland basin: Timing of the southernmost Patagonian Andes orogeny revised by detrital zircon provenance analysis. *Geology* 31, 1081–1084.

Fildani, A., and Hessler, A. M. (2005). Stratigraphic record across a retroarc basin inversion: Rocas Verdes–Magallanes Basin. Patagonian Andes. *Geol. Soc. Am. Bull.* 117, 1596–1614.

Fosdick, J. C., Graham, S. A., and Hilley, G. E. (2014). Influence of attenuated lithosphere and sediment loading on flexure of the deep-water Magallanes retroarc foreland basin, southern Andes. *Tectonics* 33, 2505–2525. doi: 10.1002/2014tc003684

Fosdick, J. C., Romans, B. W., Fildani, A., Bernhardt, A., Calderon, M., and Graham, S. A. (2011). Kinematic evolution of the Patagonian retroarc fold-and-thrust belt and Magallanes foreland basin, Chile and Argentina, 51°30'S. *Geol. Soc. Am. Bull.* 123, 1679–1698. doi: 10.1130/b30242.1

Fowler, J. N., and Novakovic, L. (2018). Deepwater slope valley reservoir architecture and connectivity. Brazil. *Lead. Edge* 37, 276–282. doi: 10.1190/tle37040276.1

Gales, J. A., Talling, P. J., Cartigny, M. J. B., Hughes Clarke, J., Lintern, G., Stacey, C., et al. (2019). What controls submarine channel development and morphology of deltas entering deep-water fjords? *Earth. Surf. Pro. Landforms* 44, 535–551. doi: 10.1002/esp.4515

Gallardo, R. E. (2014). Seismic sequence stratigraphy of a foreland unit in the Magallanes-Austral basin, Dorado Riquelme Block, Chile: implications for deep-marine reservoirs. *Lat. Am. J. Sed. Basin Anal.* 21, 49–64.

Galloway, W. E. (1989). Genetic stratigraphic sequences in basin analysis 1. Architecture and genesis of flooding-surface bounded depositional units. *AAPG Bull.* 73, 125–142.

Gerber, T. P., Pratson, L. F., Wolinsky, M. A., Steel, R., Mohr, J., Swenson, J. B., et al. (2008). Clinoform progradation by turbidity currents: modeling and experiments. *J. Sed. Res.* 78, 220–238. doi: 10.2110/jsr.2008.023

Gomis-Cartesio, L. E., Pyatotos-More, M., Hodgson, D. M., and Flint, S. S. (2018). Shelf-margin clinothem progradation, degradation and readjustment: Tanqua Depocentre, Karoo Basin (South Africa). *Sedimentology* 65, 809–841. doi: 10.1111/sed.12406

Graham, S. A., Dickinson, W. R., and Ingersoll, R. V. (1975). Himalayan-Bengal model for flysch dispersal in the Appalachian-Ouachita system. *Bull. Geol. Soc. Am.* 86, 273–286.

Hage, S., Cartigny, M. J. B., Clare, M. A., Sumner, E. J., Vendettuoli, D., Hughes Clarke, J. E., et al. (2018). How to recognize crescentic bedforms formed by supercritical turbidity currents in the geologic record: insights from active submarine channels. *Geology* 46, 563–566. doi: 10.1130/g40095.1

Hajek, E. A., and Straub, K. M. (2017). Autogenic sedimentation in clastic stratigraphy. *Ann. Rev. Earth Plan. Sci.* 45, 681–709. doi: 10.1146/annurev-earth-063016-015935

Hedberg, H. D. (1970). Continental margins from viewpoint of the petroleum geologist. *AAPG Bull.* 54, 3–43.

Helland-Hansen, W. (1992). Geometry and facies of Tertiary clinothems, Spitsbergen. *Sedimentology* 39, 1013–1029. doi: 10.1111/j.1365-3091.1992.tb01994.x

Henriksen, S., Helland-Hansen, W., and Bullimore, S. (2011). Relationships between shelf-edge trajectories and sediment dispersal along depositional dip and strike: a different approach to sequence stratigraphy. *Basin Res.* 23, 3–21. doi: 10.1111/j.1365-2117.2010.00463.x

Hodgson, D. M., Browning, J. V., Miller, K. G., Hesselbo, S. P., Poyatos-More, M., Mountain, G. S., et al. (2018). Sedimentology, stratigraphic context, and implications of intrashelf bottomset deposits, offshore New Jersey. *Geosphere* 14, 95–114. doi: 10.1130/ges01530.1

Hodgson, D. M., Kane, I. A., Flint, S. S., Brunt, R. L., and Ortiz-Karpf, A. (2016). Time-transgressive confinement on the slope and the progradation of basin-floor fans: implications for the sequence stratigraphy of deep-water deposits. *J. Sed. Res.* 86, 73–86. doi: 10.2110/jsr.2016.3

Houseknecht, D. W., Bird, K. J., and Schenk, C. J. (2009). Seismic analysis of clinoform depositional sequences and shelf–margin trajectories in Lower Cretaceous (Albian) strata, Alaska North Slope. *Basin Res.* 21, 644–654. doi: 10.1111/j.1365-2117.2008.00392.x

Houseknecht, D. W., and Shank, C. J. (2004). "Sedimentology and Sequence Stratigraphy of the Cretaceous Nanushuk, Seabee, and Tuluvak Formations exposed on Uniat Mountain, north-central Alaska," in *U.S. Geological Survey Professional Paper 1709-B*, (North-Central Alaska: USGS).

Hubbard, S. M., Covault, J. A., Fildani, A., and Romans, B. W. (2014). Sediment transfer and deposition in slope channels: deciphering the record of enigmatic deep-sea processes from outcrop. *Bull. Geol. Soc. Am.* 126, 857–871. doi: 10.1130/b30996.1

Hubbard, S. M., Fildani, A., Romans, B. W., Covault, J. A., and McHargue, T. R. (2010). High-relief slope clinoform development: insights from outcrop, Magallanes Basin, Chile. *J. Sed. Res.* 80, 357–375. doi: 10.2110/jsr.2010.042

Hubbard, S. M., Romans, B. W., and Graham, S. A. (2008). Deep-water foreland basin deposits of the Cerro Toro Formation, Magallanes Basin,

Chile: architectural elements of a sinuous basin axial channel belt. *Sedimentology* 55, 1333–1359. doi: 10.1111/j.1365-3091.2007.00948.x

Jackson, A., Stright, L., Hubbard, S. M., and Romans, B. W. (2019). Static connectivity of stacked deep-water channel elements constrained by high-resolution digital outcrop models. *AAPG Bull.* 103, 2943–2973. doi: 10.1306/03061917346

Jobe, Z. R., Bernhardt, A., and Lowe, D. R. (2010). Facies and architectural asymmetry in a conglomerate-rich submarine channel fill, Cerro Toro Formation, Sierra Del Toro, Magallanes Basin, Chile. *J. Sed. Res.* 80, 1085–1108. doi: 10.2110/jsr.2010.092

Johannessen, E. P., and Steel, R. J. (2005). Shelf-margin clinoforms and prediction of deepwater sands. *Basin Res.* 17, 521–550. doi: 10.1111/j.1365-2117.2005.00278.x

Jones, G. E. D., Hodgson, D. M., and Flint, S. S. (2013). Contrast in the process response of stacked clinothems to the shelf-slope rollover. *Geosphere* 9, 299–316. doi: 10.1130/ges00796.1

Jones, G. E. D., Hodgson, D. M., and Flint, S. S. (2015). Lateral variability in clinoform trajectory, process regime, and sediment dispersal patterns beyond the shelf-edge rollover in exhumed basin margin-scale clinothems. *Basin Res.* 27, 657–680. doi: 10.1111/bre.12092

Kane, I. A., and Hodgson, D. M. (2011). Sedimentological criteria to differentiate submarine channel levee subenvironments: exhumed examples from the Rosario Fm. (Upper Cretaceous) of Baja California, Mexico, and the Fort Brown Fm. (Permian), Karoo basin, S. Africa. *Mar. Pet. Geo.* 28, 807–823. doi: 10.1016/j.marpetgeo.2010.05.009

Kertznus, V., and Kneller, B. (2009). Clinoform quantification for assessing the effects of external forcing on continental margin development. *Basin Res.* 21, 738–758. doi: 10.1111/j.1365-2117.2009.00411.x

Kominz, M. A., Browning, J. V., Miller, K. G., Sugarman, P. J., Mizintseva, S., and Scotese, C. R. (2008). Late Cretaceous to Miocene sea-level estimates from the New Jersey and Delaware coastal plain coreholes: an error analysis. *Basin Res.* 20, 211–226. doi: 10.1111/j.1365-2117.2008.00354.x

Laskowski, A. K., DeCelles, P. G., and Gehrels, G. E. (2013). Detrital zircon geochronology of Cordilleran retroarc foreland basin strata, western Canada. *Tectonics* 32, 1–22.

Leppe, M., Mihoc, M., Varela, N., Stinnesbeck, W., Mansilla, H., Bierma, H., et al. (2012). Evolution of the Austral-Antarctic flora during the Cretaceous: new insights from a paleobiogeographic perspective. *Rev. Chile. De hist. Nat.* 85, 369–392. doi: 10.4067/s0716-078x2012000400002

Macauley, R. V., and Hubbard, S. M. (2013). Slope channel sedimentary processes and stratigraphic stacking, Cretaceous Tres Pasos Formation slope system, Chilean Patagonia. *Mar. Petrol. Geol.* 41, 146–162. doi: 10.1016/j.marpetgeo.2012.004

MacEachern, J. A., and Bann, K. L. (2008). "The role of ichnology in refining shallow marine facies models," in *Recent Advances in Models of Siliciclastic Shallow-Marine Stratigraphy*, Vol. 90, eds G. J. Hampson, R. J. Steel, P. M. Burgess, and R. W. Dalrymple, (Tulsa: Society for Sedimentary Geology Special Publication), 73–116. doi: 10.2110/pec.08.90.0073

MacEachern, J. A., Bann, K. L., Bhattacharya, J. P., and Howell, C. D. (2005). "Ichnology of deltas: Organism responses to the dynamic interplay of rivers, waves, storms, and tides," in *River Deltas – Concepts, Models, and Examples*, Vol. 83, eds L. Giosan, and J. P. Bhattacharya, (Tulsa, PA: Society for Sedimentary Geology Special Publication), 49–85. doi: 10.2110/pec.05.83.0049

Macellari, C. E., Barrio, C. A., and Manassero, M. J. (1989). Upper Cretaceous to Paleocene depositional sequences and sandstone petrography of southwestern Patagonia (Argentina and Chile). *J. S. Am. Earth Sci.* 2, 223–239. doi: 10.1016/0895-9811(89)90031-x

Madof, A. S., Harris, A. D., and Connell, S. D. (2016). Nearshore along-strike variability: is the concept of the systems tract unhinged? *Geology* 44, 315–318. doi: 10.1130/g37613.1

Malkowski, M. A., Schwartz, T. M., Sharman, G. R., Sickmann, Z. T., and Graham, S. A. (2017). Stratigraphic and provenance variations in the early evolution of the Magallanes-Austral foreland basin: implications for the role of longitudinal versus transverse sediment dispersal during arc-continent collision. *Bull. Geol. Soc. Am.* 129, 349–371. doi: 10.1130/b31549.1

Manriquez, L. M. E., Lavina, E. L. C., Fernandez, R. A., Trevisan, C., and Leppe, M. A. (2019). Campanian-Maastrichtian and Eocene stratigraphic architecture, facies analysis, and paleoenvironmental evolution of the northern Magallanes

Basin (Chilean Patagonia). *J. S. Am. Earth Sci.* 93, 102–118. doi: 10.1016/j.jsames.2019.04.010

Martinsen, O. J., and Helland-Hansen, W. (1995). Strike variability of clastic depositional systems: does it matter for sequence-stratigraphic analysis? *Geology* 23, 439–442.

Mayall, M. J., Yielding, C. A., Oldroyd, J. D., Pulham, A. J., and Sakurai, S. (1992). Facies in a shelf-edge delta – An example from the subsurface of the Gulf of Mexico, middle Pliocene, Mississippi Canyon, Block 1091. *AAPG Bull.* 76, 435–448.

McMillen, K. J. (1991). "Seismic stratigraphy of Lower Cretaceous foreland basin submarine fans in the North Slope, Alaska," in *Seismic Facies and Sedimentary Processes of Submarine Fans and Turbidite Systems*, eds P. Weimer, and M. H. Link, (New York: Springer-Verlag), 289–302. doi: 10.1007/978-1-4684-8276-8_15

Mitchum, R. M., Vail, P. R., and Thompson, S. III (1977). "Seismic stratigraphy and global changes of sea level; Part 2, The depositional sequence as a basic unit for stratigraphic analysis," in *Seismic Stratigraphy; Applications to Hydrocarbon Exploration*, Vol. 26, ed. C. E. Payton, (Tulsa, PA: AAPG), 53–62.

Muto, T., and Steel, R. J. (2002). Role of autoretreat and *A/S* changes in the understanding of deltaic shoreline trajectory: a semi-quantitative approach. *Basin Res.* 14, 303–318. doi: 10.1046/j.1365-2117.2002.00179.x

Muto, T., Steel, R. J., and Swenson, J. B. (2007). Autostratigraphy: a framework norm for genetic stratigraphy. *J. Sed. Res.* 77, 2–12. doi: 10.2110/jsr.2007.005

Mutti, E., and Normark, W. R. (1987). "Comparing examples of modern and ancient turbidite systems: problems and concepts," in *Deep Water Clastic Deposits: Models and Case Histories*, eds J. K. Legget, and G. G. Zuffa, (London: Graham and Trotman), 1–38. doi: 10.1007/978-94-009-3241-8_1

Natland, M. L., Gonzalez, E., Canon, A., and Ernst, M. (1974). A system of stages for correlation of Magallanes Basin sediments. *Mem. Geol. Soc. Am.* 139:126.

Nelson, C. H., and Kulm, L. D. (1973). "Submarine fans and channels," in *Turbidites and Deep-Water Sedimentation*, eds G. V. Middleton, and A. J. Bouma, (Tulsa, PA: Society for Sedimentary Geology), 39–70.

Nemec, W., Steel, R. J., Gjelberg, J., Collinson, J. D., Prestholm, E., and Øxnevad, I. E. (1988). Anatomy of collapsed and re-established delta front in Lower Cretaceous of eastern Spitsbergen: gravitational sliding and sedimentation processes. *AAPG Bull.* 72, 454–476.

Normark, W. R., Posamentier, H., and Mutti, E. (1993). Turbidite systems: state of the art and future directions. *Rev. Geoph.* 31, 91–116. doi: 10.1029/92rg02832

Olariu, C., and Bhattacharya, J. P. (2006). Terminal distributary channels and delta front architecture of river-dominated delta systems. *J. Sed. Res.* 76, 212–233. doi: 10.2110/jsr.2006.026

Olariu, C., and Steel, R. J. (2009). Influence of point-source sediment-supply on modern shelf-slope morphology: implications for interpretation of ancient margins. *Basin Res.* 21, 484–501. doi: 10.1111/j.1365-2117.2009.00420.x

Paola, C., Straub, K., Mohrig, D., and Reinhardt, L. (2009). The "unreasonable effectiveness" of stratigraphic and geomorphic experiments. *Earth Sci. Rev.* 97, 1–43. doi: 10.1016/j.earscirev.2009.05.003

Patruno, S., Hampson, G. J., and Jackson, C. A.-L. (2015). Quantitative characterization of deltaic and subaqueous clinoforms. *Earth Sci. Rev.* 142, 79–119. doi: 10.1016/j.earscirev.2015.01.004

Paumard, V., Bourget, J., Payenberg, T., Ainsworth, R. B., George, A. D., Lang, S., et al. (2018). Controls on shelf-margin architecture and sediment partitioning during a syn-rift to post-rift transition: insights from the Barrow Group (Northern Carnarvon Basin, North West Shelf, Australia). *Earth Sci. Rev.* 177, 643–677. doi: 10.1016/j.earscirev.2017.11.026

Pemberton, E. A. L., Hubbard, S. M., Fildani, A., Romans, B. W., and Stright, L. (2016). The stratigraphic expression of decreasing confinement along a deep-water sediment-routing system: outcrop example from southern Chile. *Geosphere* 12, 1–21.

Pemberton, E. A. L., Stright, L., Fletcher, S., and Hubbard, S. M. (2018). The influence of stratigraphic architecture on seismic response: reflectivity modeling of outcropping deepwater channel units. *Interpretation* 6, T783–T808.

Pinous, O. V., Levchuk, M. A., and Sahagian, D. L. (2001). Regional synthesis of the productive Neocomian complex of West Siberia: sequence stratigraphic framework. *AAPG Bull.* 85, 1713–1730.

Plink-Björklund, P., Mellere, D., and Steel, R. J. (2001). Turbidite variability and architecture of sand-prone, deep-water slopes: eocene clinoforms in the central Spitsbergen. *J. Sed. Res.* 71, 895–912. doi: 10.1306/030501710895

Plink-Björklund, P., and Steel, R. J. (2005). "Deltas on falling-stage and lowstand shelf-margins, the eocene central basin of spitsbergen: importance of sediment supply," in *River Deltas–Concepts, Models, and Examples*, Vol. 83, eds L. Giosan, and J. P. Bhattacharya, (Tulsa, PA: Society for Sedimentary Geology Special Publication), 179–206. doi: 10.2110/pec.05.83.0179

Ponce, J. J., and Carmona, N. (2011). Coarse-grained sediment waves in hyperpycnal clinoform systems, Miocene of the Austral foreland basin, Argentina. *Geology* 39, 763–766. doi: 10.1130/g31939.1

Porebski, S. J., and Steel, R. J. (2003). Shelf-margin deltas: their stratigraphic significance and relation to deepwater sands. *Earth Sci. Rev.* 62, 283–326. doi: 10.1016/s0012-8252(02)00161-7

Poyatos-Moré, M., Jones, G. D., Brunt, R. L., Hodgson, D. M., Wild, R. J., and Flint, S. S. (2016). Mud-dominated basin margin progradation: processes and implications. *J. Sed. Res.* 86, 863–878.

Poyatos-Moré, M., Jones, G. D., Brunt, R. L., Tek, D., Hodgson, D. M., and Flint, S. S. (2019). Clinoform architecture and along-strike variability through an exhumed erosional to accretionary basin margin transition. *Basin Res* 31, 920–947. doi: 10.1111/bre.12351

Prather, B. E., O'Byrne, C., Pirmez, C., and Sylvester, Z. (2017). Sediment partitioning, continental slopes and base-of-slope systems. *Basin Res.* 29, 394–416.

Reimchen, A., Hubbard, S. M., Stright, L., and Romans, B. W. (2016). Using sea-floor morphometrics to constrain stratigraphic models of sinuous submarine channel systems. *Mar. Petrol. Geol.* 77, 92–115.

Ridente, D., Foglini, F., Minisini, D., Trincardi, F., and Verdicchio, G. (2007). Shelf-edge erosion, sediment failure and inception of Bari Canyon on the Southwest Adriatic Margin (Central Mediterranean). *Mar. Geol.* 246, 208–230.

Romans, B. W., Castelltort, S., Covault, J. A., Fildani, A., and Walsh, J. P. (2016). Environmental signal propagation in sedimentary systems across timescales. *Earth Sci. Rev.* 153, 7–29.

Romans, B. W., Fildani, A., Graham, S. A., Hubbard, S. M., and Covault, J. A. (2010). Importance of predecessor basin history on the sedimentary fill of a retroarc foreland basin: provenance analysis of the Cretaceous Magallanes Basin, Chile (50-52°). *Basin Res.* 22, 640–658.

Romans, B. W., Fildani, A., Hubbard, S. M., Covault, J. A., Fosdick, J. C., and Graham, S. A. (2011). Evolution of deep-water stratigraphic architecture, Magallanes Basin, Chile. *Mar. Petrol. Geol.* 28, 612–628.

Romans, B. W., Hubbard, S. M., and Graham, S. A. (2009). Stratigraphic evolution of an outcropping continental slope system, Tres Pasos Formation at Cerro Divisadero, Chile. *Sedimentology* 56, 737–764.

Ross, W. C., Halliwel, B. A., May, J. A., Watts, D. E., and Syvitski, J. P. M. (1994). Slope readjustment: a new model for the development of submarine fans and aprons. *Geology* 22, 511–514.

Ryan, M. C., Helland-Hansen, W., Johannessen, E. P., and Steel, R. J. (2009). Erosional vs. accretionary shelf margins: the influence of margin type on deepwater sedimentation: an example from the Porcupine basin, offshore western Ireland. *Basin Res.* 21, 676–703.

Ryan, W. B., Carbotte, S. M., Coplan, J. O., O'Hara, S., Melkonian, A., Arko, R., et al. (2009). Global multi-resolution topography synthesis. *Geochem. Geoph. Geosyst* 10:Q03014. doi: 10.1029/2008GC002332

Schwartz, T. M., Fosdick, J. C., and Graham, S. A. (2017). Using detrital zircon U-Pb ages to calculate Late Cretaceous sedimentation rates in the Magallanes-Austral basin, Patagonia. *Basin Res.* 29, 725–746.

Schwartz, T. M., and Graham, S. A. (2015). Stratigraphic architecture of a tide-influenced shelf-edge delta, Upper Cretaceous Dorotea Formation, Magallanes-Austral basin, Patagonia. *Sedimentology* 62, 1039–1077.

Sharman, G. R., Hubbard, S. M., Covault, J. A., Hinsch, R., Linzer, H.-G., and Graham, S. A. (2018). Sediment routing evolution in the North Alpine Foreland Basin, Austria: interplay of transverse and longitudinal sediment dispersal. *Basin Res.* 30, 426–447.

Shultz, M. R., Fildani, A., Cope, T. D., and Graham, S. A. (2005). "Deposition and stratigraphic architecture of an outcropping ancient slope system: Tres Pasos Formation, Magallanes Basin, southern Chile," in *Submarine Slope Systems: Processes and Products*, Vol. 244, eds D. M. Hodgson, and S. S. Flint, (London: Geological Society Special Publication), 27–50.

Shultz, M. R., and Hubbard, S. M. (2005). Sedimentology, stratigraphic architecture, and ichnology of gravity-flow deposits partially ponded in a

growth-fault-controlled slope minibasin, Tres Pasos Formation (Cretaceous), southern Chile. *J. Sed. Res.* 75, 440–453.

Smith, C. H. L. (1977). *Sedimentology of the Late Cretaceous (Santonian–Maastrichtian) Tres Pasos Formation, Ultima Esperanza District, southern Chile.* M.Sc Thesis, University of Wisconsin, Madison, WI.

Steel, R. J., Carvajal, C., Petter, A. L., and Uroza, C. (2008). "Shelf and shelf-margin growth in scenarios of rising and falling sea level," in *Recent Advances in Models of Siliciclastic Shallow-Marine Stratigraphy*, Vol. 90, eds G. J. Hampson, R. J. Steel, P. M. Burgess, and R. W. Dalrymple, (Tulsa, PA: Society for Sedimentary Geology Special Publication), 47–71.

Steel, R. J., and Olsen, T. (2002). "Clinoforms, clinoform trajectory and deepwater sands," in *Sequence Stratigraphic Models for Exploration and Production: Evolving Methodology, Emerging Models and Application Histories*, eds J. M. Armentrout, and N. C. Rosen, (Tulsa, PA: Society for Sedimentary Geology Special Publication), 367–381.

Stevenson, C. J., Jackson, C. A.-L., Hodgson, D. M., Hubbard, S. M., and Eggenhuisen, J. T. (2015). Deep-water sediment bypass. *J. Sed. Res.* 85, 1058–1081.

Straub, K. M., Paola, C., Mohrig, D., Wolinsky, M. A., and George, T. (2009). Compensational stacking of channelized sedimentary deposits. *J. Sed. Res.* 79, 673–688.

Sylvester, Z., Deptuck, M. E., Prather, B. E., Pirmez, C., and O'Byrne, C. (2012). "Seismic stratigraphy of a shelf-edge delta and linked submarine channels in the northeastern Gulf of Mexico," in *Application of the Principles of Seismic Geomorphology to Continental-Slope and Base-of-Slope Systems: Case Studies from Seafloor and Near-Seafloor Analogues*, Vol. 99, eds B. E. Prather, M. E. Deptuck, D. Mohrig, B. Van Hoorn, and R. B. Wynn, (Tulsa, PA: Society for Sedimentary Geology Special Publication), 31–59.

Uličný, D., Nichols, G., and Waltham, D. (2002). Role of initial depth at basin margins in sequence architecture: field examples and computer models. *Basin Res.* 14, 347–360. doi: 10.1046/j.1365-2117.2002.00183.x

Wilson, T. J. (1991). Transition from back-arc to foreland basin development in southernmost Andes: stratigraphic record from the Ultima Esperanza District. *Chile. Bull. Geol. Soc. Am.* 103, 98–111.